27
8/16/85 JS (2) Cat 11

DR 1239-4

LBL-18526

I-22440

Lawrence Berkeley Laboratory
UNIVERSITY OF CALIFORNIA

EARTH SCIENCES DIVISION

HYDROLOGY AND GEOCHEMISTRY OF THE URANIUM MILL TAILINGS PILE AT RIVERTON, WYOMING
Part II. History Matching

T.N. Narasimhan, A.F. White, and T. Tokunaga

February 1985

Prepared for the U.S. Department of Energy under Contract DE-AC03-76SF00098

DISTRIBUTION OF THIS DOCUMENT IS UNLIMITED

LBL 18526

DISCLAIMER

This report was prepared as an account of work sponsored by an agency of the United States Government. Neither the United States Government nor any agency thereof, nor any of their employees, makes any warranty, express or implied, or assumes any legal liability or responsibility for the accuracy, completeness, or usefulness of any information, apparatus, product, or process disclosed, or represents that its use would not infringe privately owned rights. Reference herein to any specific commercial product, process, or service by trade name, trademark, manufacturer, or otherwise does not necessarily constitute or imply its endorsement, recommendation, or favoring by the United States Government or any agency thereof. The views and opinions of authors expressed herein do not necessarily state or reflect those of the United States Government or any agency thereof.

LBL--18526

DE85 016519

HYDROLOGY AND GEOCHEMISTRY OF THE URANIUM MILL TAILINGS PILE AT RIVERTON, WYOMING

PART II. HISTORY MATCHING

T. N. Narasimhan, A. F. White, and T. Tokunaga

Earth Sciences Division
Lawrence Berkeley Laboratory
University of California
Berkeley, California 94720

February 1985

This work was supported by the Assistant Secretary for Nuclear Energy, Office of Nuclear Waste Management, Division of Remedial Action Programs, of the U.S. Department of Energy under Contract DE-AC03-76SF00098.

DISTRIBUTION OF THIS DOCUMENT IS UNLIMITED

However, much more work remains to be done. Both sensivity analyses and parametric studies are necessary to bound the uncertainties involved in this complex problem. Before DYNAMIX can become a practical engineering tool, considerable work has to be done by way of model improvement, documentation, validation and benchmarking.

SUMMARY

In Part I of this series of two reports (Narasimhan et al., 1984) the observed fluid potential and geochemical characteristics in and around the inactive uranium mill tailings pile at Riverton, Wyoming were presented. The purpose of the present work is to attempt to simulate field observations using mathematical models. The results of the studies have not only helped identify the physicochemical mechanisms governing contaminant migration around the inactive mill tailings pile in Riverton, but also have indicated the feasibility of quantifying these mechanisms with the help of newly developed mathematical models. Much work needs to be done to validate and benchmark these models.

The history-matching effort on hand involves the mathematical simulation of the observed fluid potentials within the tailings, and the observed distribution of various chemical species within and around the inactive uranium mill tailings. The simulation problem involves consideration of transient fluid flow and transient, reactive chemical transport in a variably saturated ground water system with time-dependent boundary conditions.

For purposes of the present study, the overall problem was subdivided into three stages. Stage 1 consisted of modeling the time-dependent infiltration of water through the tailings since abandonment, taking into account evapotranspiration and rainfall boundary conditions. This was accomplished using the computer program TRUST; the computed disposition of fluid potentials within the tailings agreed reasonably well with observed values.

Stage 2 of the present study, which is concerned with the mixing of tailings water and ground water, required the greatest amount of effort and innovation. The basic requirement was to simulate the simultaneous migration of several

chemical species, duly considering precipitation of supersaturated phases and the dissolution of buffering species in the solid matrix. For this purpose, a new program, DYNAMIX, was developed by coupling a generalized version of program TRUMP with the geochemical speciation code, PHREEQE. Using this model, ten chemical species, namely, Ca, Mg, Na, K, Fe, Si, Al, C, Cl and SO_4 were transported by advection, dispersion and diffusion mechansims. The precipitation and dissolution of gypsum, iron hydroxide, gibbsite and calcite were considered. An explicit scheme of marching in the time-domain was followed. The tailings-aquifer interaction was modeled in a quasi-three-dimensional fashion. The results of the mixing calculation yielded reasonable agreement with observed data in regard to pH as well as sulfate in the shallow aquifer immediately beneath the tailings. These calculations also yielded the precipitation rate of gypsum over the life of the tailings.

The purpose of the last stage was to use the observed ground water velocity, the infiltration rate and the rate of precipitation of gypsum in a two-dimensional areal model of the aquifer, and to simulate the sulfate plume that extends from the tailings southeast to the Little Wind River. For this purpose, the TRUMP computer program was used. In this model, the precipitation rates for gypsum, calculated with the DYNAMIX code in Stage 2, became the known, time-dependent sink terms. To simplify the handling of hydrodynamic dispersion, the mesh was oriented in the direction parallel to the approximate direction of regional groundwater flow, NW-SE. The plume calculated with the numerical model agreed surprisingly well with observed data, considering the complexity of the problem.

The results generated so far can be used as a first approximation to forecast the possible response of the system to alternate remedial scenarios.

TABLE OF CONTENTS

LIST OF FIGURES iv

LIST OF TABLES vi

NOMENCLATURE vii

ACKNOWLEGEMENT ix

INTRODUCTION 1

METHODOLOGY 8

The Problem 8
The Approach 8
The Tools 11
The Codes TRUST and TRUMP 11
Program DYNAMIX 11
Governing Equations 11
Titration and Precipitation 15
Program PHREEQUE 18

RESULTS 20

Stage I: The Infiltration Problem 20
Hydraulic Head Profiles Observed in the Field 21
Atmospheric Conditions 26
Arbitrary Fixed Fluid Potential 26
Coupled Climate/Surface Potential Dependent Evaporation Model 28
The Complementary Relationship Areal Evaporation Method (CRAE) 28
Two-Dimensional Vertical Transect Simulation 38

Stage 2: Multiple Species Transport 44
The Dilution Front Problem 44
The Lower Interphase Leaching Problem 47
The Tailings - Aquifer Mixing Problem 52

Stage 3: The Contaminant Pluma Problem 60

DISCUSSION 67

REFERENCES 70

LIST OF FIGURES

Fig. 1.	Location map of the Riverton, Wyoming mill tailings site.	2
Fig. 2.	Vertical profiles of fluid potential within tailings at Riverton, Site RB.	3
Fig. 3.	Disposition of water table at the Riverton site on November 3, 1982.	4
Fig. 4.	Vertical profiles of major and minor elements at site RB, Riverton.	5
Fig. 5.	Dispositions of different chemical plumes, Riverton: (a) sulfate, (b) uranium, (c) molybdenum, (d) pH.	6
Fig. 6.	Three-stage sequential approach to history matching.	10
Fig. 7.	Sketch of an arbitrary elemental volume.	13
Fig. 8.	Schematic of flow region modeled in the three stages.	19
Fig. 9.	One dimensional discretization for infiltration problem.	23
Fig. 10.	Soil properties used in simulation of Stage 1:	
	a) Saturation versus pressure head	24
	b) Hydraulic conductivity versus pressure head.	25
Fig. 11.	Results of simulation: step-changed surface potentials.	27
Fig. 12.	Results of simulation: evapotranspiration by the method of Staple.	30
Fig. 13.	Evapotranspiration estimates by the CRAE method of Morton.	32
Fig. 14.	Results of simulation: using CRAE method and 44 rainfall events per year.	34
Fig. 15.	Results of simulation: recharge to water table by various techniques.	36
Fig. 16.	Results of simulation: profiles of potential using CRAE method with quarterly averaged sink-source terms.	37
Fig. 17.	Results of simulation: two-dimensional E-W transect; normal water table.	40
Fig. 18.	Results of simulation: two-dimensional E-W transect; high water table.	41
Fig. 19.	Results of simulation: two-dimensional E-W transect; impermeable cover over tailings.	43

Fig. 20.	Results of simulation: dilution front; comparison of effects of two different infiltration rates.	45
Fig. 21.	Results of simulation: comparison of simulated and observed dilution profiles.	48
Fig. 22.	Geometric set up used for analyzing the possible flushing out of lower part of tailings.	49
Fig. 23.	Schematic of mesh used in the tailings-aquifer mixing calculations.	53
Fig. 24.	Infiltration rate as a function of time used in tailings-aquifer mixing calculations.	56
Fig. 25.	Results of simulation: sulfate profile as a function of time within aquifer below the tailings.	58
Fig. 26.	Results of simulation: precipitation rates of sulfate as a function of time.	59
Fig. 27.	Mesh used for sulfate plume simulation.	61
Fig. 28.	Results of simulation: sulfate plume as a function of time.	63
Fig. 29.	Results of simulation: comparison of simulated and observed sulfate plumes.	64
Fig. 30.	Results of simulation: comparison of simulated (20m moles/liter) and observed (21 mmoles/liter) sulfate contours.	65

LIST OF TABLES

Table 1. Mean monthly climatic data summary for Riverton Wyoming, 1972-1981. 29

Table 2. Chemical compositions of tailings water and rain water. 46

Table 3. Chemical compositions of ground water and tailings water. 54

NOMENCLATURE

b	Designation for a large volume element which is used to simulate a boundary condition	$[M/L^3]$
c^i	Concentration of ith species	$[M/L^3]$
c^i_ℓ	Concentration of ith species in volume element ℓ	$[M/L^3]$
$\bar{c}^i$	Time averaged concentration of ith species at an interface	$[M/L^3]$
$c^i_{\ell,m}$ $c^i_{\ell b}$	Concentration of ith species at the interface between volume element ℓ and volume element m or b	$[M/L^3]$
Δc^i_ℓ	Change in concentration of ith species in volume element ℓ	
D_d	Molecular diffusion coefficient	$[L^2/T]$
D_H	Hydrodynamic dispersion coefficient	$[L^2/T]$
D_{ij}	Components of hydrodynamic dispersion tensor	$[L^2/T]$
$F_{\ell m}$, $F_{\ell b}$	Volumetric flux into volume element ℓ from volume element m or b	$[L^3/T]$
G^i	Rate of dissolution (+) or precipitation (-) of species i	$[M/T]$
G^i_ℓ	Rate of dissolution (+) or precipitation (-) of species i in volume element ℓ	$[M/T]$
K	Hydraulic conductivity	$[L/T]$
K^i_d	Retardation coefficient with respect to ith species	$[L^3/M]$
ℓ	Designation of a volume element	
m	Designation of a volume element	
n	Porosity	[1]
q	Darcy velocity or specific flux	$[L/T]$
Δt	Time interval	
$S_{w,\ell}$	Water saturation in volume element ℓ	[1]
v	Pore velocity	$[L/T]$

$V_{B,\ell}$	Bulk volume of volume element ℓ	$[L^3]$
$V_{w,\ell}$	Volume of water in volume element ℓ	$[L^3T]$
z	Elevation	$[L]$
α_L	Longitudinal dispersivity	$[L]$
α_T	Transverse dispersivity	$[L]$
Γ_ℓ	Closed surface bounding volume element ℓ	$[L^2]$
$d\Gamma$	A segment of Γ_ℓ	$[L^2]$
$\Delta\Gamma_{\ell m}, \Delta\Gamma_{\ell b}$	Area of interface between element ℓ and element m or b	$[L^2]$
∇	Gradient operator	
λ_d^i	Radioactive decay constant for ith species	$[1/T]$
ρ_{dry}	Dry bulk density of geologic material	$[M/L^3]$
ϕ	Hydraulic head or fluid potential, head of water	$[L]$
ψ	Pressure head, head of water	$[L]$

INTRODUCTION

The basic outcome of the first part (Narasimhan et al., 1984) of this two-part report was establishment of the following features, based on field data from the Uranium Mill Tailings Site at Riverton, Wyoming (Fig. 1).

- The profiles of fluid potentials within the partially saturated tailings as a function of time (Fig. 2);
- The physical properties of the tailings and soil materials, including porosity, permeability, fluid saturation, and the dependencies of permeability and fluid saturation on capillary pressure head;
- The disposition of the water table within the aquifer as a function of time (Fig. 3);
- The geochemical profiles within the tailings, including pH, Ca, Mg, Na, K, Fe, Al, SiO_2, Cl, SO_4, U and Mo (Fig. 4);
- The disposition of the plumes of SO_4, U, pH, and Mo within the shallow aquifer (Fig. 5).

The next logical step in the overall investigations is to establish the cause-effect connection between the history of the milling activities at the site and the present day hydrogeochemical situation as detailed above. This "history-matching" effort is critical to the ultimate objective of the UMTRAP program for the following reason: successful history matching will identify the hydrological and chemical processes that control the contaminant migration at the Riverton site; the prediction of the contaminant distribution behavior under various plausible remedial scenarios will have to be based on the processes that control contaminant migration.

The purpose of the history-matching effort, which is the content of this report, is to use mathematical models and quantitatively explain the present hydrogeochemical situation at Riverton as a consequence of what happened at the site between 20 and 25 years ago, during the active phase of the mill. The goal is to simulate, using the physical parameters

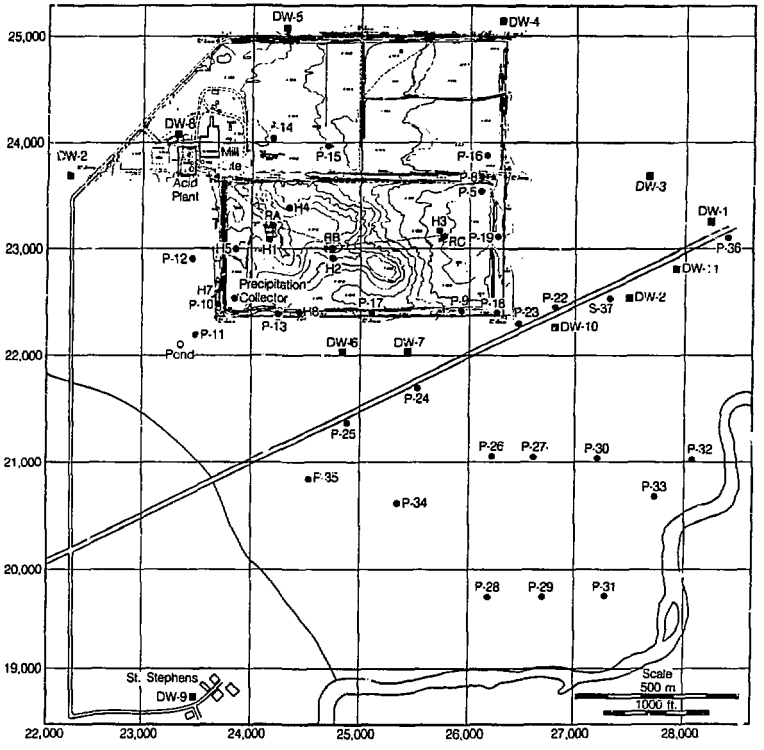

Fig. 1. Location map of the Riverton, Wyoming Mill Tailings site.

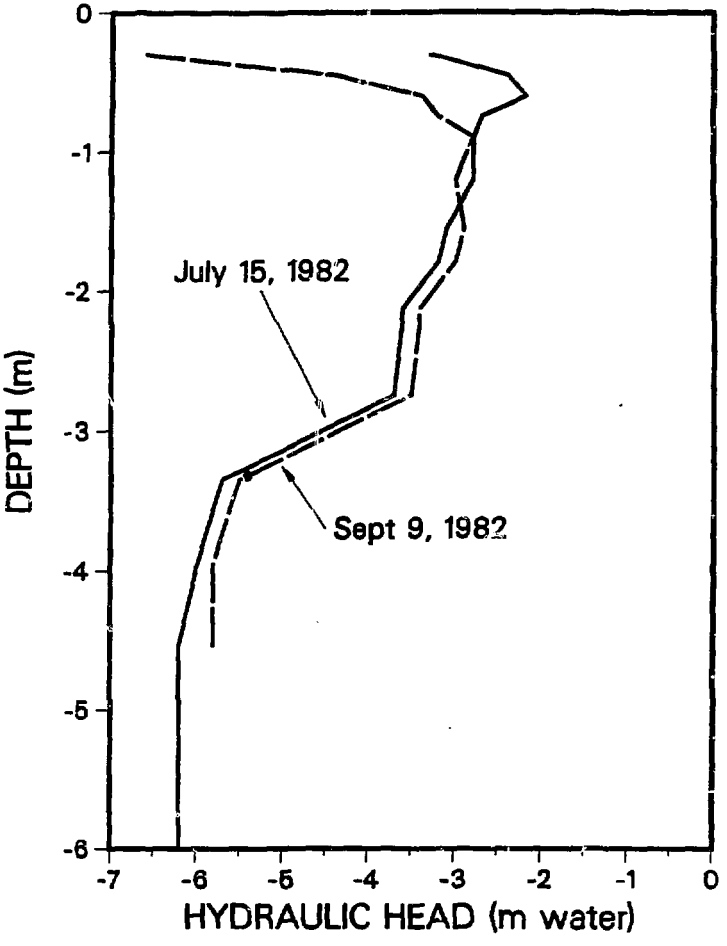

XCG 837-7221

Fig. 2. Vertical profiles of fluid potential within tailings at Riverton, Site RB.

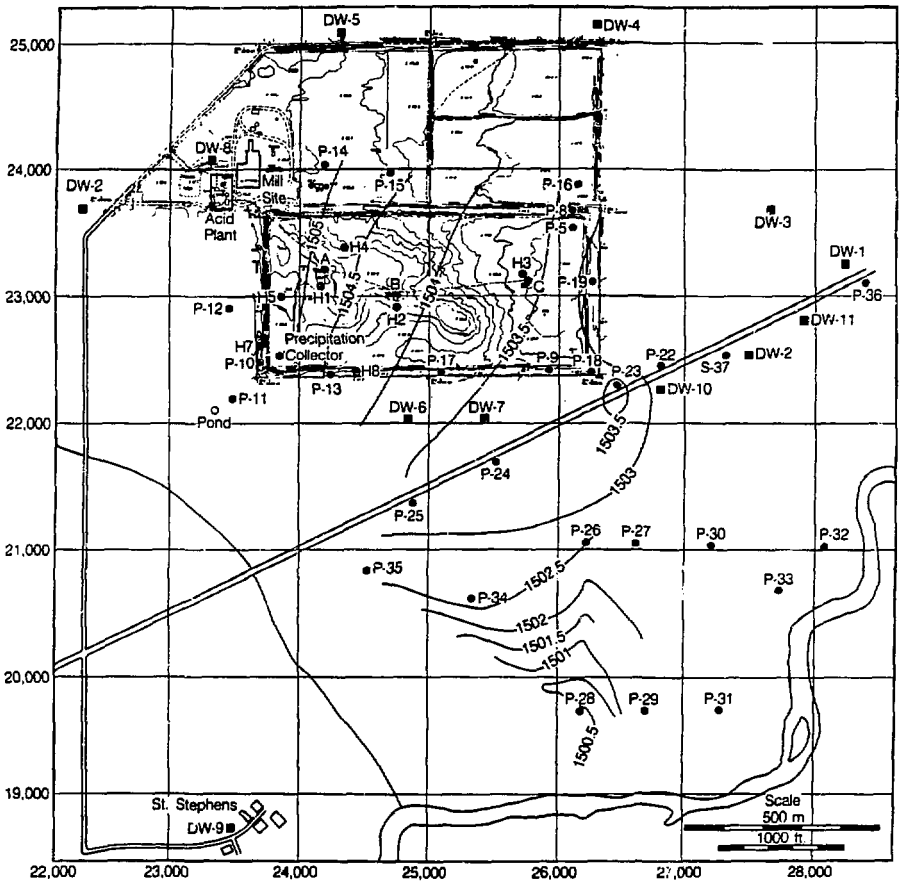

Fig. 3. Disposition of water table at the Riverton site on November 3, 1982.

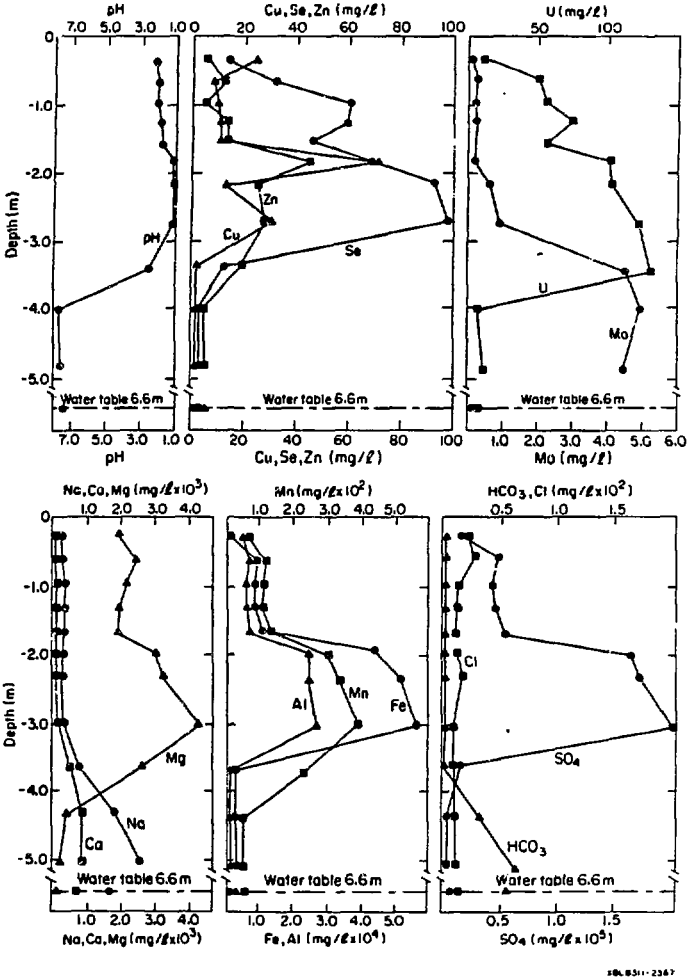

Fig. 4. Vertical profiles of major and minor elements at site RB, Riverton.

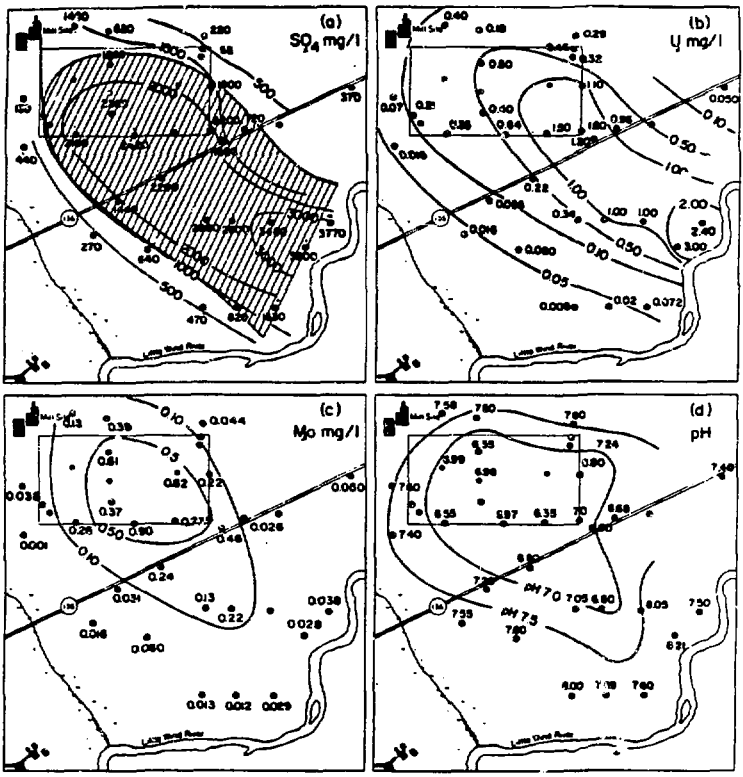

XBL 8311-7392C

Fig. 5. Dispositions of different chemical plumes, Riverton: (a) sulfate, (b) uranium, (c) molybdenum, (d) pH.

observed in the field and in the laboratory, the observed profiles of fluid potentials and geochemical profiles within the tailings, and the deposition of the sulfate plume within the shallow aquifer. The extension of the history matching results to predictive calculations for the future is beyond the scope of the present report.

METHODOLOGY

In this section we discuss the philosophy and the tools that are necessary to analyze the field problem. The discussions are divided into three parts: statement of the problem, discussion of the approach, and description of the tools.

THE PROBLEM

The transport of contaminants from the tailings pile to the ground water system is governed by the dynamics of the water phase. In addition to advective transport, which includes both advection and hydrodynamic dispersion, molecular diffusion is also an important transport mechanism. Therefore, a prerequisite for analyzing the chemical transport problem is knowledge of the dynamics of fluid flow as well as the distribution of fluid saturations within the tailings pile. Secondly, the transport process is greatly influenced by the chemical interactions that take place when the highly acidic tailings water mixes with the near neutral ground water in the presence of a soluble solid phase such as calcite. Thus, the overall problem is one of transient fluid flow and transient chemical transport in a three-dimensional, partially saturated to fully saturated, heteogeneous system.

THE APPROACH

At the present time, many reliable mathematical tools are available to handle transient fluid flow and transient transport of a single reactive chemical species. However, no tools are currently available to handle the simultaneous transport of several reacting chemical species and the resultant precipitation-dissolution phenomena. Therefore, a new mathematical tool, a computer model, was developed to handle the multiple species transport problem involved in the dynamic mixing of the tailings water with the shallow

ground water. The new model DYNAMIX, in conjunction with other models already available, led to a sequential three-stage history-matching effort schematically shown in Figure 6.

The purpose of Stage 1 is to obtain the transient infiltration rates through the tailings since the time of their emplacement. These infiltration rates will determine the quantity of tailings water that has entered the ground water system. The infiltration rates thus constitute an essential input to Stage 2. The purpose of Stage 2 is to carry out the dynamic mixing of the tailings water and the ground water, involving several chemical species, and to carry out the migration of the dilution front in the upper part of the tailings. This stage, which involves the newly developed tool DYNAMIX, is computationally quite time-consuming, even on a large main-frame computer. At present, we are able to handle only a few tens of grid blocks with reasonable expenditure of computer time. Therefore, the simulation of multiple species transport over the entire plume area is not computationally feasible. To overcome this, we restrict the multiple species simulations to the portion of the shallow aquifer immediately below the tailings. The outcome is the transient evolution of aqueous chemical concentrations of the various chemical species within the shallow aquifer below the tailings, as well as the transient precipitation and dissolution rates of the specific mineral phases - calcite, gypsum, gibbsite and iron hydroxide. Using this output, we set for ourselves the limited goal, in Stage 3, of simulating the evolution of the plume of just one species, namely, sulfate.

The outcome of each of the three stages is finally compared with the corresponding field measurements summarized in Figures 2 through 5, which is a measure of the success of the history-matching effort.

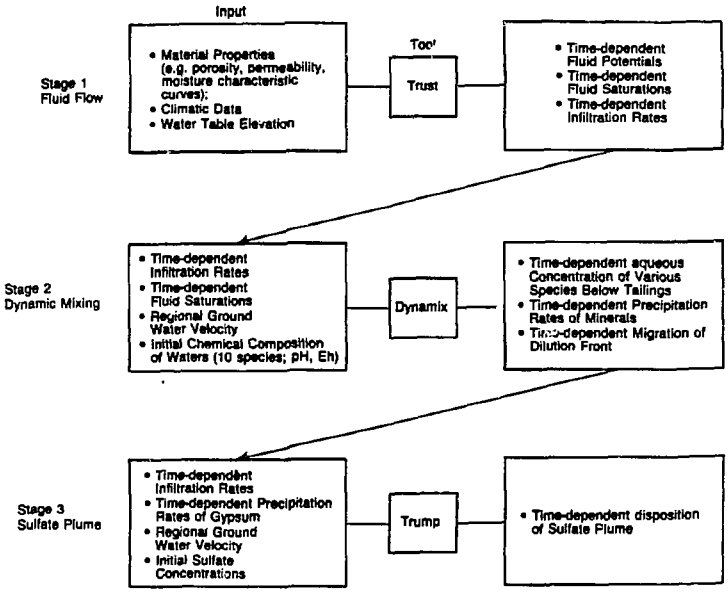

Fig. 6. Three-stage sequential approach to history matching.

THE TOOLS

The tools of history-matching used in the present work are all numerical models (TRUST, TRUMP, DYNAMIX) based on the Integral Finite Difference Method (Narasimhan and Witherspoon, 1976). The models all handle flow in three dimensions, and can account for heterogeneities, time-dependent sources, time-dependent boundary conditions and arbitrary initial conditions.

The Codes TRUST and TRUMP

The TRUST code solves for isothermal fluid flow in variably saturated porous media, fractured media or fractured porous media. The theoretical basis, the algorithm and the application of TRUST are described, respectively, in a series of three papers in Water Resources Research (Narasimhan and Witherspoon, 1977; Narasimhan et al., 1978; Narasimhan and Witherspoon, 1978). The application of TRUST specifically to uranium mill tailings is given in Reisenauer et al. (1982), along with a user's guide.

The TRUMP code (Edwards, 1972) solves for transient and steady state temperature distributions in the presence of advection and diffusion. One can use the TRUMP code directly for chemical transport problems by simply recognizing the similarities between the heat transport equation and the chemical transport equation (e.g., Rasmuson et al., 1982).

For details regarding TRUST and TRUMP the reader is referred to the references given above. In the interest of space and time we will not describe these codes here.

Program DYNAMIX

Governing Equations

DYNAMIX (DYNamic MIXing), is a multiple species, advective-dispersive chemical transport model which accounts for aqueous geochemical interactions between the chemical species. This algorithm was developed by

extending TRUMP to handle several species and combining with it the aqueous geochemistry code PHREEQE (Parkhurst et al., 1980).

The thrust of the DYNAMIX Code is to solve the following advective-dispersive-diffusive chemical transport equation for an arbitrary elemental volume ℓ, which is fully enclosed by the closed surface Γ_ℓ (Fig. 7). This equation expresses the mass conservation of the ith chemical species in the aqueous phase.

$$-\int_{\Gamma_\ell} \vec{q}\cdot\vec{n}\, d\Gamma\, \bar{c}^i + \int_{\Gamma_\ell} nD_H \vec{\nabla} c^i \cdot \vec{n}\, d\Gamma + \int_{\Gamma_\ell} nD_d^i \nabla c^i \cdot \vec{n}\, d\Gamma$$

$$+ G^i - V_{w,\ell}\, \lambda_d^i \left(1 + \frac{\rho_{dry}}{n}\right) K_d^i\, c_\ell^i = V_{w,\ell} \left(1 + \frac{\rho_{dry}}{n}\right) K_d^i\, \frac{\Delta c_\ell^i}{\Delta t} \qquad (1)$$

where

$\vec{q}$ = the darcy velocity at the surface segment $d\Gamma$ [L/T]

$\vec{n}$ = unit outer-normal to the surface segment $d\Gamma$

$\bar{c}^i$ = average concentration of the ith species at the surface $d\Gamma$ [M/L^3]

c_ℓ^i = average concentration of the ith species in element ℓ [M/L^3]

$d\Gamma$ = segment of the bounding surface Γ_ℓ [L^2]

Γ_ℓ = closed surface bounding element ℓ [L^2]

n = porosity

D_H = hydrodynamic dispersion coefficient [L^2/T]

D_d = effective molecular diffusion coefficient [L^2/T]

G^i = source/sink term: $G^i > 0$ denotes dissolution and is a source. $G^i < 0$ denotes precipitation and is a sink [M/T].

λ_d^i = decay constant for the ith species [1/T]

$V_{w,\ell}$ = volume of water in element ℓ [L^3]

ρ_{dry} = dry bulk density of the porous material [M/L^3]

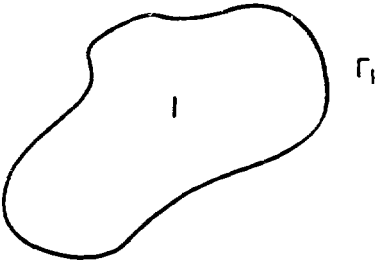

XBL 8411-6264

Fig. 7. Sketch of an arbitrary elemental volume.

K_d = distribution coefficient or partition coefficient (Freeze and Cherry, 1979) $[L^3/M]$

Δt = interval of time.

For the Riverton problem we shall ignore adsorption and radioactive decay by setting $K_d = 0$ and $\lambda_d = 0$ in Equation (1).

If we discretize the system in such a fashion that the volume element is bounded by stream lines and isopotential lines, the required discretized governing equation is

$$\sum_m F_{\ell m}\,\bar{c}^i_{\ell m} + \sum_b F_{\ell b}\bar{c}^i_{\ell b} + \sum_m nD_H\vec{\nabla}c^i\cdot\vec{n}\Delta\Gamma_{\ell m} + \sum_b nD_H\vec{\nabla}c^i\cdot\vec{n}\,\Delta\Gamma_{\ell b}$$

$$+ \sum_m nD_d\vec{\nabla}c\cdot n\vec{\Delta\Gamma}_{\ell m} + \sum_b nD_d\vec{\nabla}c\cdot\vec{n}\Delta\Gamma_{\ell m} + G^i_\ell = V_{w,\ell}\,\frac{\Delta c^i_\ell}{\Delta t} \qquad (2)$$

where

m denotes a surface segment that is entirely interior to the flow region

b denotes a surface segment that lies entirely on the external boundary of the flow region.

$F_{\ell m}$, $F_{\ell b}$ are volumetric water fluxes into element ℓ across an interior surface $\Delta\Gamma_{\ell m}$ or an exterior surface $\Delta\Gamma_{\ell b}$.

The indicated summations over b are designed to take care of all boundary conditions. The fluid fluxes $F_{\ell m}$ and $F_{\ell b}$ are obtained either from Stage 1 calculations using TRUST or from known regional ground water flow conditions at the site. Because we shall define the volume element to be bounded by stream lines and isopotential surfaces, we may define D_H as follows:

$$D_H = \begin{cases} \alpha_L\,|v|\,, & \text{if } \Delta\Gamma_{\ell m} \text{ is perpendicular to stream lines} \\ \alpha_T\,|v|\,, & \text{if } \Delta\Gamma_{\ell m} \text{ is parallel to stream lines} \end{cases} \qquad (3)$$

where

α_L = longitudinal dispersivity [L]

α_T = transverse dispersivity [L]

v = pore velocity [L/T]

Furthermore, since hydrodynamic dispersion causes spreading only along the direction of fluid flow, such dispersive spreading cannot occur in the direction that is upstream with reference to fluid flow. On the other hand, molecular diffusion can cause diffusive flux in any direction, regardless of the fluid flow direction. Therefore, for computing solute flux due to longitudinal dispersion, we shall impose the following constraint:

$$nD_L \frac{\Delta c^i}{\Delta x} \Delta\Gamma_{\ell m} = \begin{cases} 0, & \text{if } c^i_{upstream} < c^i_{downstream} \\ >0, & \text{if otherwise} \end{cases} \tag{4}$$

We will assume that for the partially saturated zone,

$$V_{w,\ell} = V_{B,\ell}\, n\, S_{w,\ell} \tag{5}$$

where

$V_{B,\ell}$ = the bulk volume of element ℓ

n = porosity of the material

$S_{w,\ell}$ = fluid saturation.

Titration and Precipitation

We now need to consider the source/sink term in Equations (1) and (2). In our problem the term G^i_ℓ arises when the water contained in ℓ mixes with the incoming water of different chemical composition, leading to precipitation or dissolution. The mixing is also supplemented by additional flux into the element ℓ of the different species due to dispersion and diffusion. We now idealize this mixing of waters of different chemical composition as a titration process in which the mixture is well stirred at all times.

Physically, the stirring mechanism in our case is provided by hydrodynamic dispersion and molecular diffusion. For a chosen interval of time, Δt, the size of the elemental volume should be small enough that the mixing process can influence the entire element.

For purposes of mixing, we need to consider two separate incoming chemical fluxes: advective flux and diffusive flux. We will now restrict ourselves to sufficiently small time steps, Δt, so that the transient calculations can be carried out explicitly (Narasimhan et al., 1978). Using the explicit technique for marching in the time domain, we implement the mixing calculations as follows. First, the diffusive and the dispersive solute fluxes are added to element ℓ by evaluating the 3rd through 6th terms on the left hand side of Equation (2). Then the advective mixing (titration) is carried out by considering each interface $\Delta\Gamma_{\ell m}$ separately. For simplicity, the concentration of the incoming fluid with reference to any species is taken to be that of the upstream node (full upstream weighting). That is, $\bar{c}^i_{\ell m}$ taken to be equal to c^i_{up}, the concentration at the upstream nodal point Volumetrically, the mixing is done at constant volume $V_{w,\ell}$. That is, $(F_{\ell m}\,\Delta t)$ cubic units of the incoming fluid with concentration c^i_{up} are mixed with $V_{w,\ell} - F_{\ell m}\Delta t$ cubic units of the water in element ℓ with concentration c^i_ℓ.

The titration is carried out in the program PHREEQE, which has been incorporated in DYNAMIX as a series of subroutines. After the titration process is completed with respect to all the surface segments bounding ℓ, the resulting electrolyte is checked for its saturation state with reference to specific mineral species of interest. Based on this, the titrated solution is equilibrated with the specific minerals for which supersaturation

exists, as well as with any buffering mineral phase, such as calcite, that may occur in the element ℓ. This equilibration process results in the precipitation of the supersaturated mineral species and the dissolution of the buffer mineral.

The sequential steps involved in DYNAMIX are as follows:

STEP 1: Charge-balance the initial solution.

STEP 2: For every time step carry out the following for each elemental volume:

(a) Explicitly compute the change in concentration due to diffusion and dispersion.

(b) Perform titration of the advecting flux with the fluid in the element. Set the concentration of the incoming fluid to that of the upstream element. Titrate $F_{\ell m}\Delta t$ cubic units of incoming fluid with $V_{w,\ell} - F_{\ell m}\Delta t$ cubic units of fluid in element ℓ after (a) has been carried out.

(c) Check the titrated solution for saturation with respect to specified mineral species of interest.

(d) Equilibrate the solution with those minerals with which the solution is found to be supersaturated. Also include, in the equilibration process, any buffering mineral that is known to exist in the solid phase.

STEP 3: Calculate the final concentration of the aqueous phase at the end of Δt.

Compute the quantity of precipitation of dissolution of the appropriate mineral phases.

In the present work, we are concerned with the following ten species: Ca, Mg, Na, K, Fe, Aℓ, Si, Cℓ, C (total alkalinity), and SO_4. In addition, pH and Eh are also an integral part of the calculations. The mineral phases of interest are gypsum, gibbsite and iron hydroxide. We assume, based on field observations (Narasimhan et al., 1984) that the shallow aquifer consists of an abundance of calcite, which acts as a buffer in the chemical reactions. Therefore, the titrated solution is automatically equilibrated against calcite in Step 2.

The titration calculations and the equilibration calculations were carried out with the PHREEQE subroutines, by repeatedly calling them from the transport subroutines.

Program PHREEQE

At this point it is pertinent to give a brief description of program PHREEQE. The PHREEQE code (Parkhurst et al., 1980) is a FORTRAN IV computer code designed to model geochemical reactions. The aqueous model, which includes chemical elements, aqueous species, and mineral phases, is exterior to the computer code and is completely user definable. PHREEQE can simulate several types of reactions, including: (i) addition of reactants; (ii) mixing of two waters; (iii) titration of one solution with another. The program calculates the following quantities during the reaction simulation: pH; pe; the total concentration of elements; the amounts of minerals in other phases transferred into and out of solution; the distribution of aqueous species; and the saturation state of the aqueous phase with respect to specified mineral phases.

A detailed discussion of the application of the PHREEQE code to describe chemical contamination by the Riverton mill tailings pile is presented by White et al. (1984). The flow regions modeled in each of the three stages and their mutual relationships are depicted schematically in Figure 8.

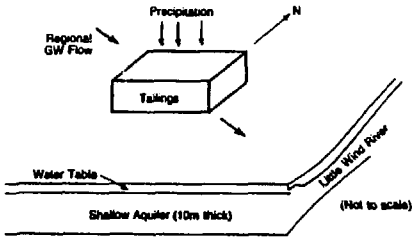

Idealization of Tailings — Ground Water System for Mathematical Modeling

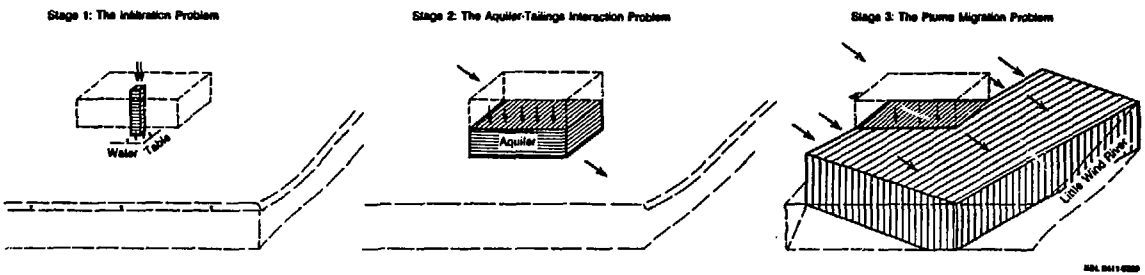

Fig. 8. Schematic of flow region modeled in the three stages.

RESULTS

STAGE 1: THE INFILTRATION PROBLEM

In order to understand the processes governing the observed contamination of the shallow aquifer underlying the tailings pile, evaluation of water inflow from the contaminant source is required. To achieve this goal, numerical simulations of flow within the tailings were performed from a variety of approaches, using the integrated finite difference program TRUST (Narasimhan et al., 1978). Since field observations indicate that the bulk of the tailings water undergoes vertical flow through partially saturated tailings, the majority of the simulations were performed for one-dimensional columns. The one-dimensional modeling focused on simulating conditions at site RB in the Riverton tailings pile (see Part 1, Fig. 3). This choice was based on the fact that site RB is the centrally located monitoring station, considered representative of most of the pile. The one-dimensional simulations were conducted using three different approaches for handling the evapotranspiration boundary conditions at the upper surface of the tailings. Characterizing the upper boundary condition is the most difficult component of our one-dimensional simulations, since the upper surface is subject to wide, and often rapid changes in potential and water saturation. The water table underlying the one-dimensional column remained at a relatively constant level with an annual fluctuation of less than about 1 m, and therefore was modeled as a fixed potential boundary in all of the simulations. Material properties characteristic of the tailings were taken from laboratory measurements of hydraulic conductivity and saturation as functions of matric (suction) head (Narasimhan et al., 1984).

The first approach to handling the tailings/atmosphere interaction utilized rather arbitrary step changes of the surface pressure/suction head to model alternating cycles of rainfall and evaporation. The second method involved

application of a model by Staple (1974), which couples local climatic conditions with evaporation dependent on surface matrix potential. The third approach considered the Complementary Relationship Areal Evaporation (CRAE) model of Morton (1978). In one application of the CRAE model, scaled-down CRAE evaporation rates were applied between individual rainstorms. In a second version, precipitation and scaled-down CRAE evaporation rates were averaged over three-month periods.

A final set of simulations of the tailings pile considered a vertical two-dimensional east-west transect through the center of the tailings. These two-dimensional simulations allow analysis for possible lateral components of flow in the deeper tailings. If lateral flow exists in significant quantity within the capillary fringe above the water table and within part of the deeper tailings within the capillary zone, then the lateral flux may perhaps account for the zone of apparent leaching observed below a depth of about 4 m at site RB (Fig. 4).

A realistic simulation of flow within the tailings must closely match field observations. Thus, the validity of all simulations is assessed from this perspective. In the following section the field measurements of hydraulic head profiles are reviewed. The details of the various simulations are then presented.

Hydraulic Head Profiles Observed in the Field

This discussion focuses on site RB of the Riverton tailings pile, which is the central monitoring site. The hydraulic head profiles at site RA are in many ways similar to those of site RB (Narasimhan et al., 1984), while the measurements at site RC do not typify the pile as a whole. Thus the hydraulic head profiles at site RB are assumed to be representative of the tailings pile.

As noted in Part I of this report (Narasimhan et al., 1984) and elsewhere (Tokunaga and Narasimhan, 1982) the hydraulic head gradients at site RB are relatively stable within the tailings at depths greater than 1 m below the upper surface (Fig. 2). Within 1 m of the upper surface, wide fluctuations in hydraulic head are observed in response to rainfall and evaporation events. Below this surface zone the bulk of the tailings appear to exhibit relatively steady unsaturated downward flow towards the shallow water table. The profiles reflect a roughly unit hydraulic head gradient directed downward at both sites RA and RB. At site RB a lens of relatively low permeability tailings is observed at a depth of about 3 m, within which the hydraulic head gradient is substantially larger in magnitude. Throughout the bulk of the steady-state region the matric (suction) head is observed in the range of -2 to -1 m H_2O. At site RB the water table is about 6.7 m below the upper surface and about 2 m below the tailings soil interface. Tokunaga and Narasimhan (1982) obtained an estimated range of steady recharge rates from ranges of laboratory measured/calculated unsaturated hydraulic conductivities (for $\bar{\psi}$ = -1.5 m H_2O), combined with a unit hydraulic head gradient. This range of recharge rates is equivalent to an annual recharge of about 3×10^{-3} to 3×10^{-2} m of water. The simulations to be described are checked for the extent to which the steady portion of the hydralic head profiles are matched. Rates of shallow aquifer recharge are also monitored in the simulations.

A schematic representation of the one-dimensional set up is given in Figure 9. The material properties used in the simulations are given in Figure 10a and b.

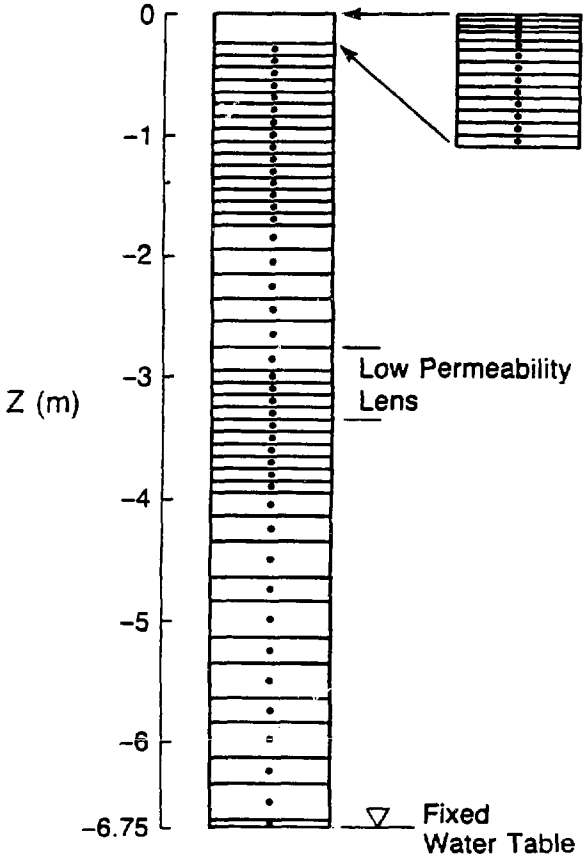

XBL 8411-6265

Fig. 9. One dimensional discretization for infiltration problem.

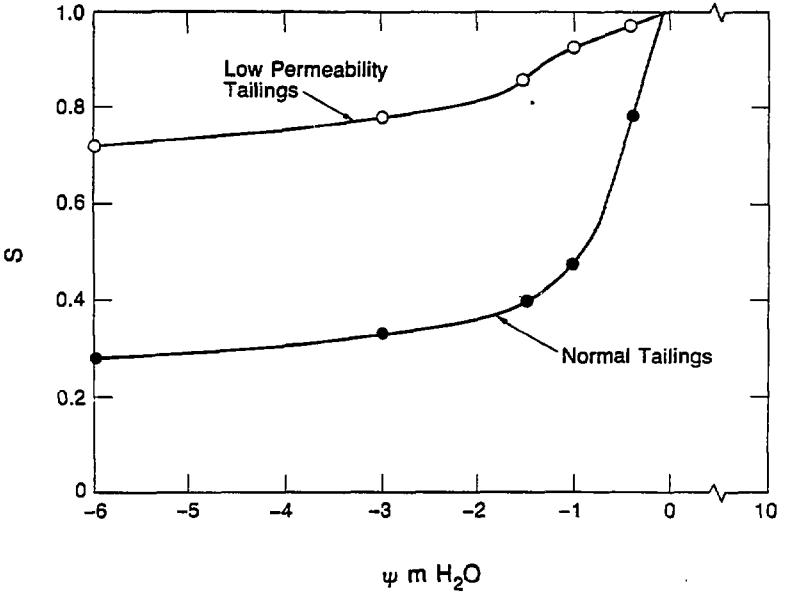

XBL 8411-6263

Fig. 10a. Soil properties used in simulation of Stage 1: Saturation versus pressure head.

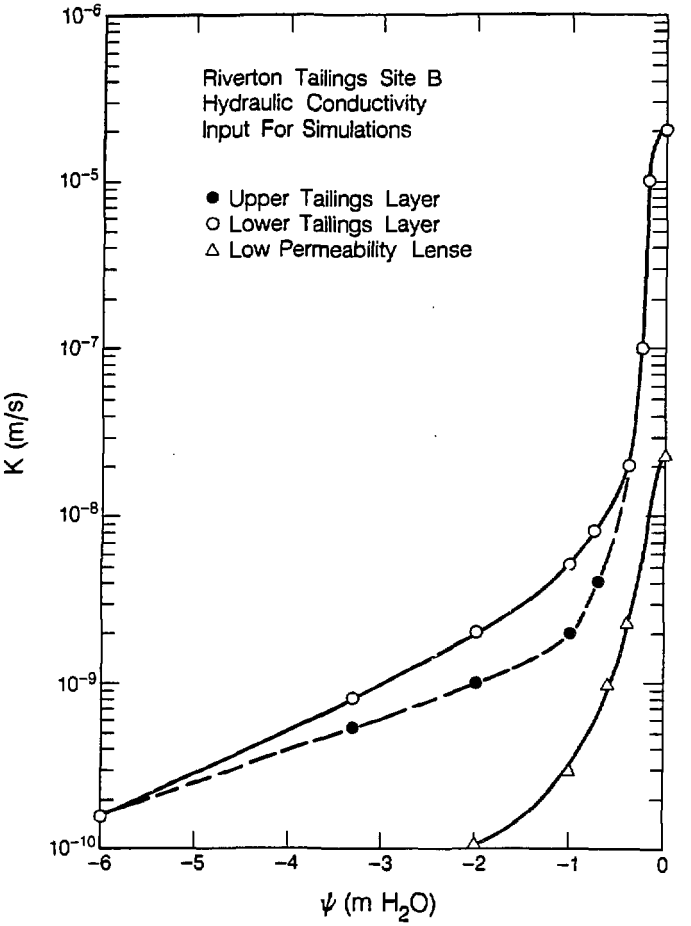

Fig. 10b. Soil properties used in simulation of Stage 1: Hydraulic conductivity versus pressure head.

Atmospheric Boundary Conditions

Techniques of varying complexity are available to handle the evapotranspiration conditions at the tailings surface. In our study we have tried three different techniques: (i) use of arbitrary surface potentials, (ii) the method of Staple (1974), and (iii) the method of Morton (1978).

Arbitrary Fixed Fluid Potential

The preliminary model consisted of a vertical set of volume elements with the lowest node (volume element) connected to a fixed potential surface (the water table) and the uppermost node connected to a time-dependent surface potential. The latter boundary potential alternated between -6.0 and 0.001 m of water to simulate evaporation and rainfall events, respectively. The evaporation and rainfall periods were, respectively, 0.1 year and 6 hours. Nine and one half of these cycles comprised each simulated year. The duration of the rain period was selected to be consistent with the Riverton mean annual precipitation of 0.2 m. By extending this simulation to 10 years, a quasi-steady-state hydraulic head profile was generated through the bulk of the tailings. The simulated profile is very similar to the one observed in the field (Fig. 11). The steady state recharge of the ground water in the tailings simulation at the end of 10 years is 0.03 m per year, which is consistent with the earlier estimates of Tokunaga and Narasimhan (1982).

Although this model has yielded credible results, its chief deficiency is that it is based on arbitrarily chosen magnitudes and durations of the surface potentials. The two following approaches aim to avoid this deficiency by utilizing available climatological data from the vicinity of the Riverton tailings. For this purpose, climatological data from the Riverton and the Lander, Wyoming weather stations were collected for the ten-year period 1972-1981 and compiled into monthly averages.

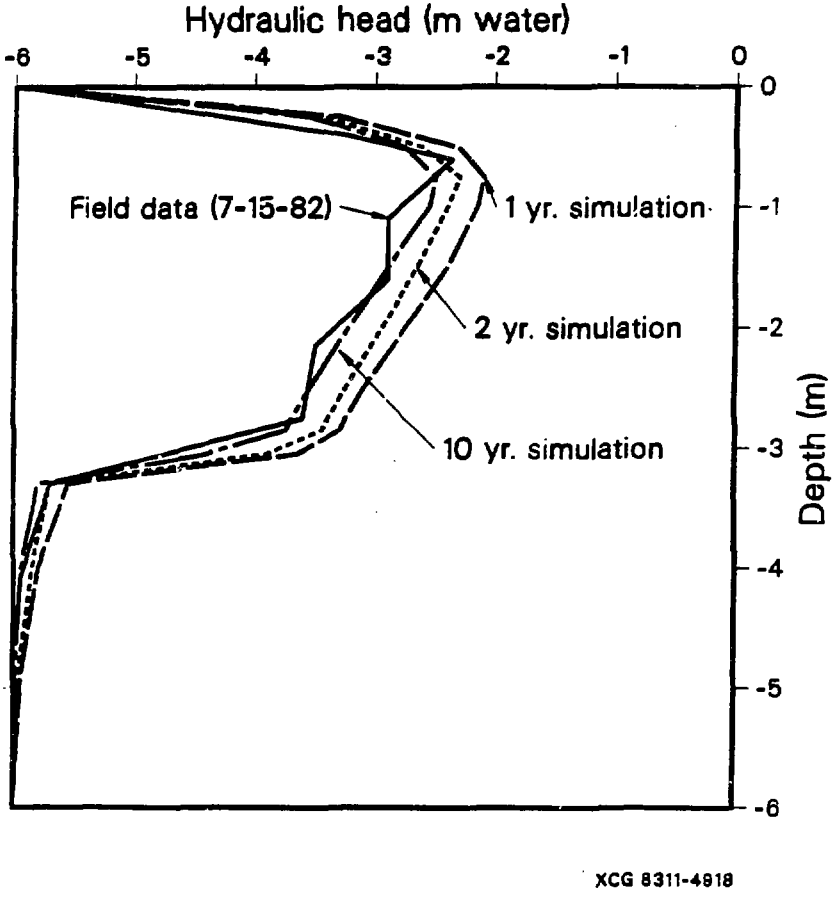

Fig. 11. Results of simulation: step-changed surface potentials.

Coupled Climate/Surface Potential Dependent Evaporation Model

The method of Staple (1974) effectively substitutes the surface soil water vapor pressure for the saturation vapor pressure in the Penman potential evaporation equation. Climatic data compiled in Table 1 were used to generate monthly averaged evaporation functions for surface sinks dependent on potentials. An assumption used in this application of the Staple method is that the magnitude of the surface water potential is largely determined by the surface matric (suction) potential. Rainfall was concentrated into 0.005 m events via 2-hour durations of a 0.0025 m/hr surface source. The 44 events distributed over the year were designed to nominally follow monthly averaged rainfall patterns at Riverton. The simulation was carried out for three years following an initial condition of full saturation.

The outcome of using the Staple method is that a net loss of fluid is calculated at the surface. This net loss can only be accounted for by depleting the moisture stored within the tailings. This is reflected in the hydraulic head profiles depicted in Figure 12. The zero-flux internal boundary continues to migrate well into the body of the tailings, well below its position observed in the field. Several attempts using alternative selections of rainfall intensities and magnitudes did not appreciably change the net moisture loss at the surface. These observations are contradictory to the field observations, which clearly show net surface gains of rain water.

The Complementary Relationship Areal Evaporation Method (CRAE)

The Complementary Relationship Areal Evaporation method (CRAE) of Morton (1978) was the third approach used to estimate evaporation losses from the

Table 1. Mean monthly climatic data summary for Riverton, Wyoming, 1972-1981.

	Jan	Feb	Mar	Apr	May	Jun	Jul	Aug	Sep	Oct	Nov	Dec
Precipitation (cm)	.43	.53	1.25	2.97	4.32	4.17	1.55	.91	1.91	1.96	1.17	.53
Air temperature (°C)	-9.4	-4.9	-0.2	6.6	12.2	16.7	21.1	19.9	14.0	7.6	-1.5	-7.7
Relative humidity	.68	.63	.57	.53	.52	.42	.39	.40	.42	.52	.63	.65
Wind speed ($km \cdot day^{-1}$)	220	224	282	297	309	328	301	286	270	228	212	232
* $\frac{n}{N}$	.61	.65	.66	.64	.62	.75	.75	.75	.77	.65	.56	.58
+ R_A $\frac{cal}{cm^2 day}$	280	430	660	790	940	990	960	830	640	510	320	250
Soil temperature (°C at 1 m)	3.6	1.9	2.5	5.6	8.9	12.5	16.1	18.3	16.8	13.9	10.0	6.3

* $\frac{n}{N}$ is the actual duration of bright sunshine per maximum possible

+ R_A is the maximum upper atmosphere radiation at 43°N latitude (List, 1951)

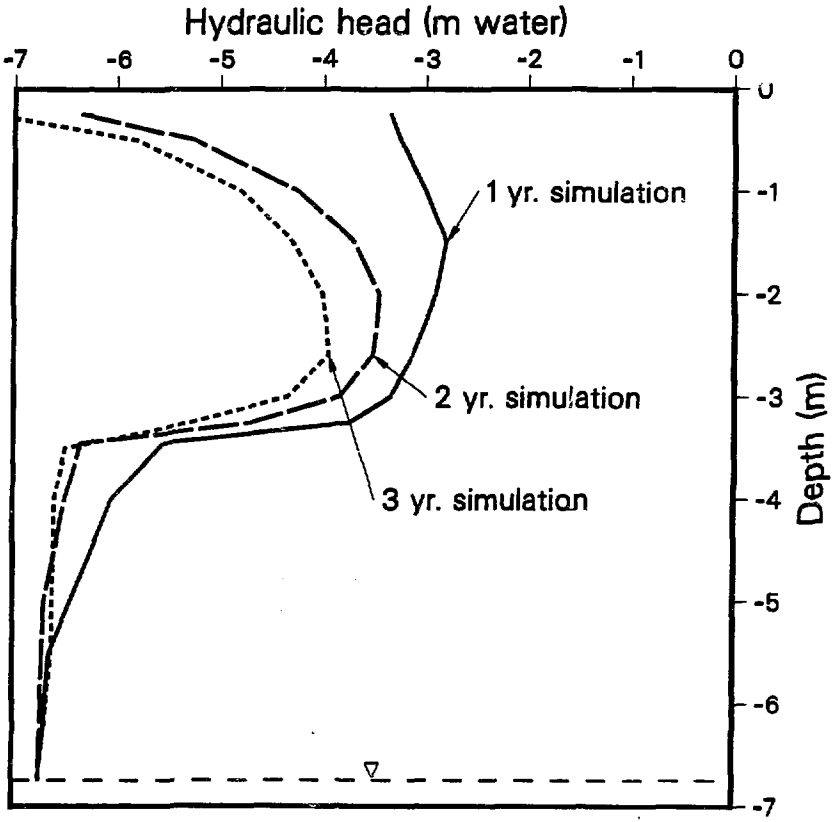

XCG 8311-4919

Fig. 12. Results of simulation: evapotranspiration by the method of Staple.

Riverton tailings. Monthly averaged climatic data again were used. Because the method involves a large set of equations, only the results of the calculations are discussed in the interest of space. Figure 13 shows monthly evaporation losses in cm, as well as monthly averaged precipitation. Results of the Staple method are included for comparison. Although the CRAE method also predicts net evaporation losses, the magnitudes of such losses are clearly smaller than those of the Staple method. It should be pointed out here that the CRAE method is a model for regional evaporation. Therefore the CRAE results presented in Figure 13 more likely reflect the Riverton region as a whole. The actual evaporation losses at the Riverton site may be much smaller than this average. Therefore, with reasonable estimates of the deviation of the tailings surface evaporation from the typical surface of the Riverton region, the CRAE approach may prove to be a useful management tool for the Riverton tailings. It seems reasonable to expect that the sparsely vegetated, cobbly tailings cover at the Riverton site would evapotranspire at about 50% of the regional rate. This reduction would be sufficient to make the CRAE method yield results consistent with field observations.

From these considerations the CRAE monthly evaporation rates were scaled down to 55% of the full rates for use in simulating evaporation. This scales down the predicted 36.1 cm annual evaporation to 19.9 cm/yr. It should be emphasized that this is a rather arbitrary reduction of the CRAE calculations. The factor 0.55 (55%) was chosen since it leaves a net recharge of 2.1 cm/yr into the tailings. This chosen recharge rate is close to the upper limit of predicted steady recharge mentioned earlier. In principle, scaling down the original CRAE annual losses by any factor such that a slight recharge is obtained is consistent with field observed recharge. For a mean annual precipitation of 22.1 cm (which, although measured at a Riverton weather

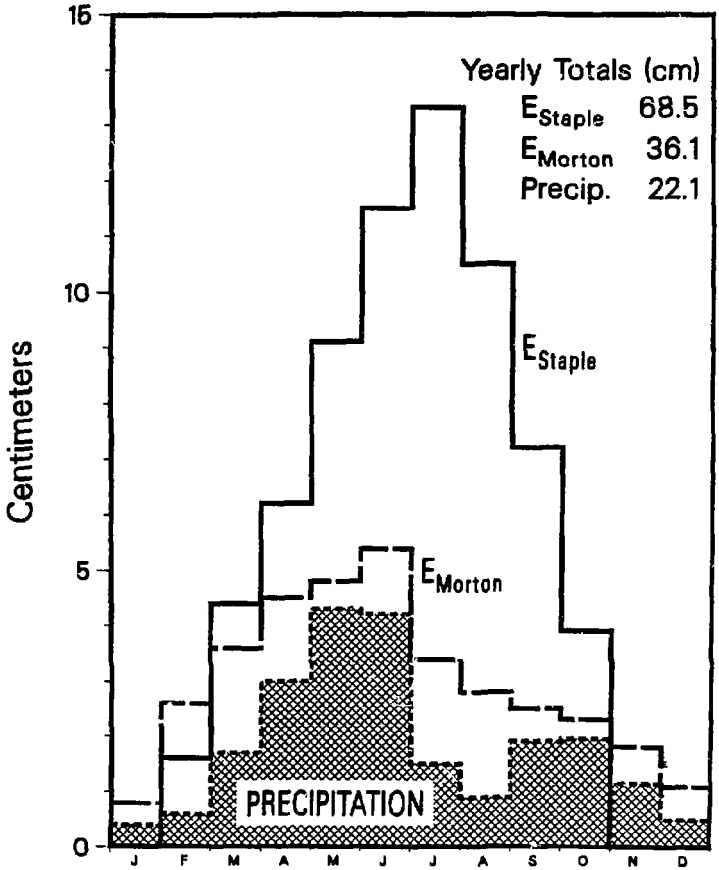

XCG 8311-4917

Fig. 13. Evapotranspiration estimates by the CRAE method of Morton.

station, may not adequately characterize precipitation on the tailings pile), the original CRAE losses can therefore be scaled down by factors of 0.61 or less.

In the first appplication of the scaled down Morton (CRAE) evaporation rates, the reduced (by a factor 0.55) monthly average evaporation rates were applied at the upper surface between individual 0.005 m rainfall events. The 44 yearly rainfall events were distributed in time to nominally correspond to the monthly average Riverton precipitation patterns. This approach will be referred to as the "detailed 0.55X CRAE" method.

The simulation of tailings fluid flow with the detailed 0.55X CRAE approach was performed for 11 years with an initial condition of a fully saturated tailings pile. The simulated hydraulic head profiles shown in Figure 14 exhibit steady-state flow at depths greater than 1 m by about the 7th year. However, the steady-state hydraulic head profiles are shifted towards zero relative to the field observed profiles, indicating a more saturated system. This comparison by itself can raise questions regarding the appropriateness of the unsaturated hydraulic conductivity functions, $K(\psi,z)$, used in the model. More specifically, this shifted $\phi(z)$ profile is associated with a $\psi(z)$ shift towards saturation. Since $K(\psi)$ increases as ψ increases (towards zero), the shifted $\phi(z)$ in the simulation suggests the possibility that the $K(\psi,z)$ relations used in the model are too low (i.e., for a given ψ, the $K(\psi)$ used is too small). However, the use of large $K(\psi)$ functions appears unjustified based on laboratory measured $K(\psi)$.

The true cause of the discrepancy between the field-measured and simulated $\phi(z)$ profiles is revealed by comparing yearly recharge at the upper surface and at the water table below. When the steady-state profiles are obtained, the

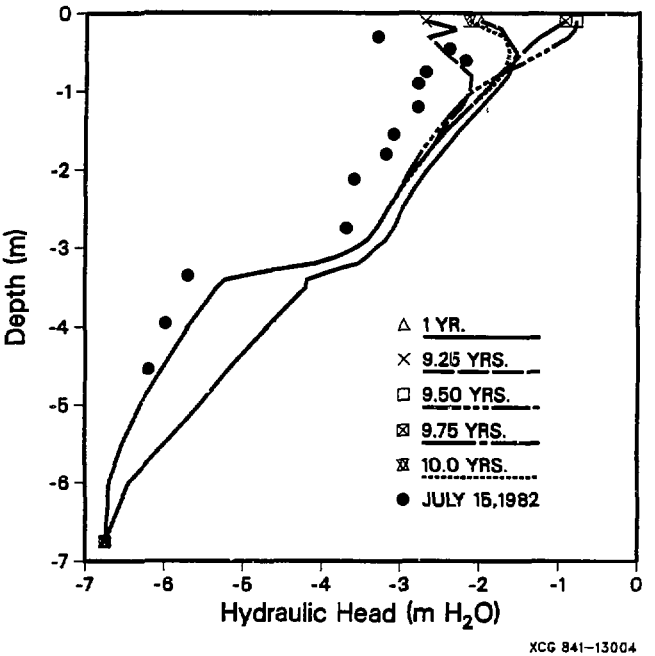

Fig. 14. Results of simulation: using CRAE method and 44 rainfall events per year.

constraint of fluid mass balance requires that the yearly recharge of the shallow aquifer becomes equal to the yearly recharge rate of 2.1 cm at the upper tailings surface. Contrary to this requirement, the detailed 0.55X CRAE model settles to an aquifer recharge rate of about 5 cm/yr. The cause of this anomaly appears to be the complexity of the problem; that is, the response of a highly non-linear system to a cyclic boundary perturbation. This is dramatically illustrated in Figure 15; the flux at the bottom of the column shows a more or less stable oscillation with time. Obviously, detailed handling of the rainfall events is not only computationally expensive, but is also beset with problems of stability.

A second approach based on a scaled-down CRAE model represents a much coarser time-averaging for the upper boundary sink/source, as well as an attempt to minimize fluid mass conservation errors associated with the detailed 0.55X CRAE model. In this second version, the precipitation and 0.55X CRAE rates are averaged together over three-month periods to obtain four lumped surface sink/source rates per year. This approach is designated the "quarterly 0.55X CRAE" method. As with the previous approaches, the initial condition was that of a fully saturated tailings pile.

Quasi-steady-state hydraulic head profiles are obtained by about the tenth year in the quarterly 0.55X CRAE approach. As shown in Figure 16, the steady-state regions of the model are very close to the field measured hydraulic head profiles. Furthermore, as seen in Figure 15, with the quarterly 0.55X CRAE method the system approaches an average aquifer recharge rate of 2.1 cm/yr. Thus, the mass balance requirement is met along with the matching of the field hydraulic head profiles.

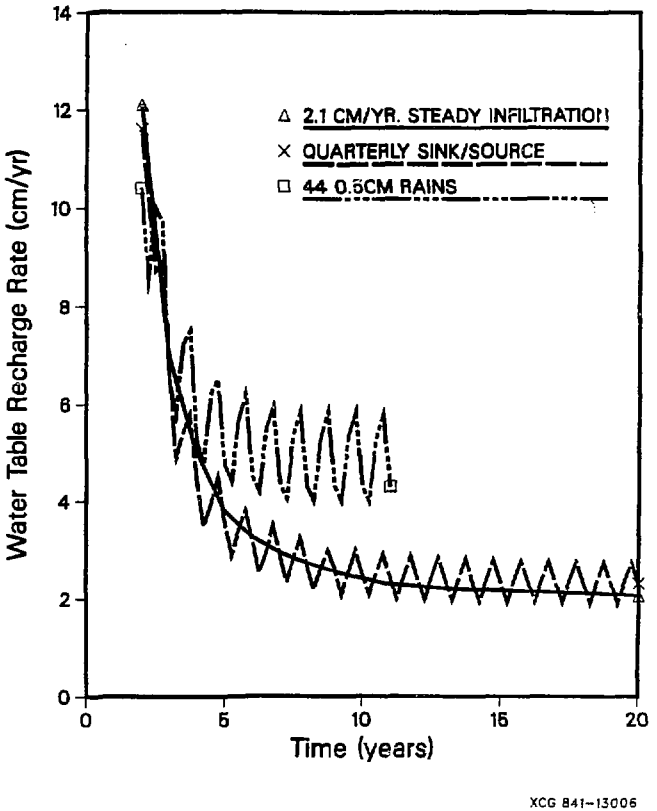

Fig. 15. Results of simulation: recharge to water table by various techniques.

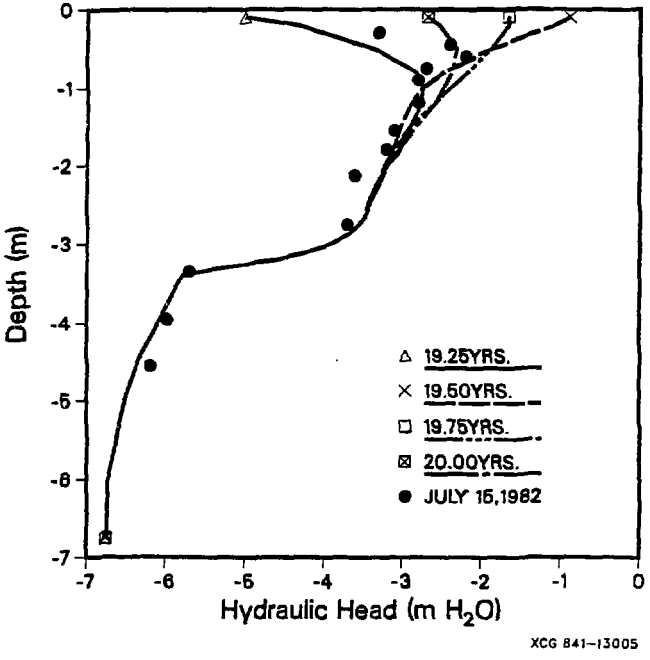

Fig. 16. Results of simulation: profiles of potential using CRAE method with quarterly averaged sink-source terms.

The aquifer recharge rates using the detailed 0.55X CRAE method as well as a steady 2.1 cm/yr surface source are also plotted in Figure 15. The anomalously high steady recharge rates from the detailed 0.55X CRAE method are quite evident. It is interesting to note that the periodic, seasonal variations at the upper surface are detectable as oscillations in the aquifer recharge rates. It is also evident that the yearly average aquifer recharge with the quarterly 0.55X CRAE model follows the pattern for the 2.1 cm/yr steady surface source quite closely.

Two-Dimensional Vertical Transect Simulation

As a final step in analyzing fluid flow patterns, a two-dimensional vertical transect through the east-west center line of the pile was modeled. A slight gradient in the water table exists, sloping downward from west to east. With this sloping potentiometric surface arises the possibility of groundwater flowing up across the water table, laterally through the tailings, and back down into the shallow aquifer at the downstream (eastern) end of the tailings pile. Discussion of this possibility can be found in Luthin and Day (1955). The transect shown in Part I of this report (Fig. 3, Narasimhan et al., 1984) was modeled as a largely homogeneous tailings pile, with 1 to 2 m of subsoil, and a shallow aquifer. A low permeability lens was used within the tailings at site RB. Steady recharge through the upper tailings surface was set at 1 cm/yr. The choice of a lower recharge rate in the two-dimensional studies was made to enhance the possibility of observing lateral components of flow within the capillary fringe. With high surface recharge rates, vertical flow is certain to dominate throughout the tailings pile. Surface recharges rates lower than about 1 cm/yr would provide simulation results which neither approximate the field hydraulic head profiles, nor allow sufficient input of neutral water to account for the

diluted upper tailings solution. The water table levels were controlled by fixing the potentials at the upstream and downstream aquifer boundaries. Simulations were performed for 1 cm/yr steady recharge with normal as well as raised water tables. A final simulation considered the effects of an impermeable surface cover (with normal water table elevations).

The steady-state profile for the tailings pile with 1 cm/yr surface recharge and normal shallow aquifer water levels is shown in Figure 17. The hydraulic heads essentially decrease vertically throughout the tailings. Lateral flow above the water table is found only in the subsoil. The lateral gradients in hydraluic head are small, being at most about 2×10^{-3} $m \cdot m^{-1}$, which is roughly the magnitude of the slope of the piezometric surface. Thus, dilution of water in the lower tailings by water from the shallow aquifer moving upward across the water table appears unlikely when water levels are near normal or lower. Before considering the other two cases, it should be noted that despite the simplicity of this model of the normal conditions, it is very consistent with field measurements. The downward-directed near-unit hydraulic head gradient measured in the tailings is reproduced in this simulation. Furthermore, the model closely matches field observations in terms of the the range of the matric (suction) head in the tailings. In both the field and model, matric (suction) head values in the range of -1.0 to -1.5 m H_2O typify the tailings. These correlations between field measurements and the model provide further support to the conclusion that no dilution of the tailings water by flow from the shallow aquifer occurs under normal conditions.

The steady-state profile of the tailings with a raised water table is shown in Figure 18. Again, a steady surface recharge of 1 cm/yr is applied. The piezometric surface in this "flooded" system nearly coincides with the

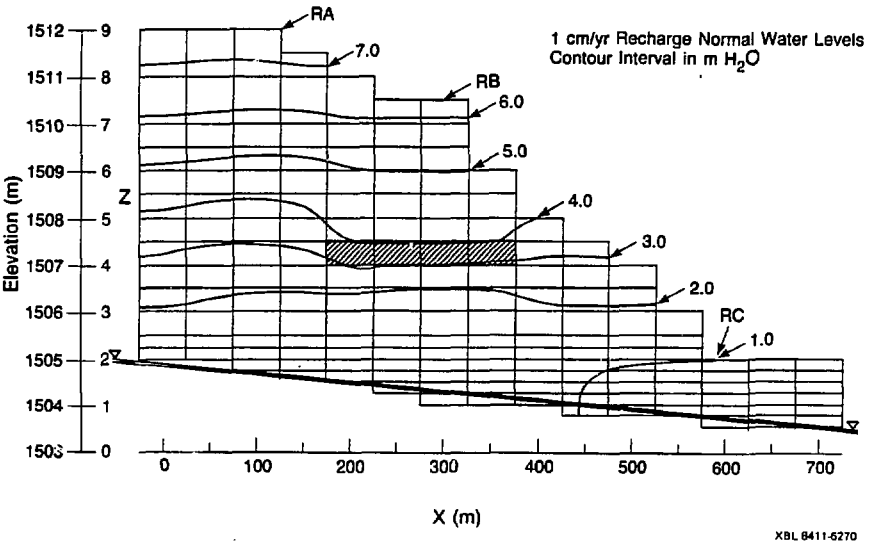

Fig. 17. Results of simulation: two-dimensional E-W transect; normal water table.

Tokunaga, T., and T. N. Narasimhan, 1982. Recent Hydrologic Observations from the Riverton and Maybell Tailing Piles, Proceedings of the Fifth Symposium on Uranium Mill Tailings Management, Colorado State University, Fort Collins, 463-474.

White, A. F., J. M. Delany, T. N. Narasimhan and A. Smith, 1984. Groundwater Contamination from an Inactive Uranium Mill Talings Pile, Part I. Application of a Chemical Mixing Model, Water Resources Res., 20(11), 1743-1752.

ACKNOWLEGEMENT

This work was supported by the Assistant Secretary for Nuclear Energy, Office of Nuclear Waste Management, Division of Remedial Action Programs, of the U.S. Department of Energy under contract DE-AC03-76SF00098. We would like to thank Mary G. Bodvarsson for editing the report and Leslie Fairbanks for word processing.

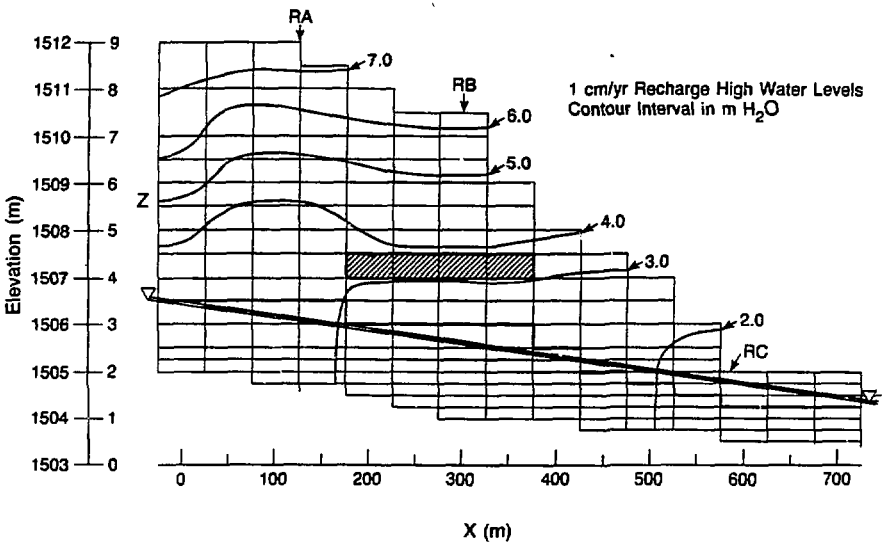

XBL 8411-6271

Fig. 18. Results of simulation: two-dimensional E-W transect; high water table.

tailings-subsoil interface. Again, flow throughout most of the tailings pile is directed vertically downward. Lateral components to tailings water flow are found only within 0.5 m of the subsoil interface. Even in this zone the magnitude of the lateral gradient is only about 3×10^{-3} $m \cdot m^{-1}$ at most. Thus, dilution of tailings water by lateral flow appears minor even in the case of high water levels. However, increases in saturation of about 15% are found in the tailings that are within 0.5 m of the subsoil in the "flooded" model. Changes in saturation drop off rapidly with increased elevation. A sequence of flooding cycles would be necessary to develop the observed diluted zone in the lower tailings if saturation changes were the primary dilution mechanism. Without long-term water level records for the site, no conclusions can be made regarding tailing water dilution by variable saturation from below the pile.

The case where the tailings pile is capped by an impermeable cover is shown in Figure 19. Normal water table levels were used in obtaining this steady-state profile. Lateral flow clearly dominates in this case. Recharge occurs solely through the upstream aquifer. Ground water then mixes with tailings water within the pile, after which the mixture is discharged downstream. Although lateral flow dominates, flow rates through the tailings are very low due to both low hydraulic head gradients and very low unsaturated hydraulic conductivities. The product of the average hydraulic gradient (0.0025 $m \cdot m^{-1}$) times a characteristic unsaturated hydraulic conductivity within the pile (8×10^{-10} $m \cdot s^{-1}$) provides a typical lateral flux density of 2×10^{-12} $m \cdot s^{-1}$ or 6×10^{-5} $m \cdot yr^{-1}$. It should be emphasized that these flow rates are not fundamentally due to the addition of the impermeable surface cover. Instead, it is the combined effect of the low local slope in the piezometric surface with low unsaturated hydraulic conductivities of the tailings which produce the very low flux densities through the pile.

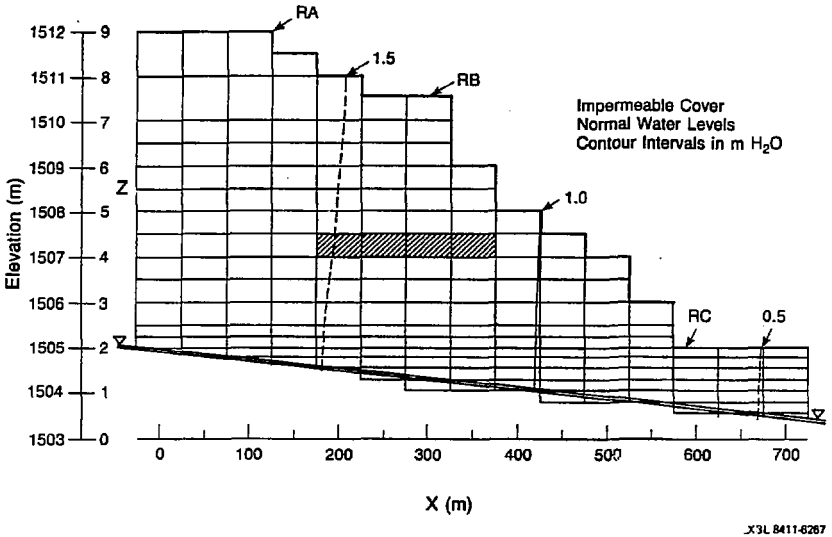

Fig. 19. Results of simulation: two-dimensional E-W transect; impermeable cover over tailings.

STAGE 2: MULTIPLE SPECIES TRANSPORT

The multiple species transport problem at the Riverton Site can be divided into three separate problems:

(a) The occurrence of a migrating dilution front within 2 m of the tailings surface, which is caused by the simple dilution of the tailings water by rain water;

(b) The presence of a prominent zone of apparent leaching below a depth of about 4 m, observed at site RB;

(c) The mixing of the tailings water and the shallow ground water across the lower interface.

The Dilution Front Problem

The upper two meters of the tailings at site RB, within which the dilution front is observed in the field, is also the region within which the flow field is highly subject to reversals of direction due to seasonal climatic changes. As such, the chemical transport within this region should be extremely complex. From a practical viewpoint, we will not address these complexities in our effort. Instead, we shall greatly simplify the system by assuming a constant average annual infiltration rate at the surface. We shall consider a one-dimensional column, 3 m tall by 1 m^2 in area. The column is divided into 15 elemental volumes, each 0.2 m thick. We assume the porosity of the tailings to be 45% and the average saturation to be 65%. The chemical composition of the rain water and the tailings water are given in Table 2.

Two cases are considered, using two different values of average annual infiltration rates: 2 cm/yr and 3 cm/yr. A comparison of the DYNAMIX results for the two cases is shown in Figure 26 at a time approximately corresponding to the present time, i.e., 20 years after abandonment of the site.

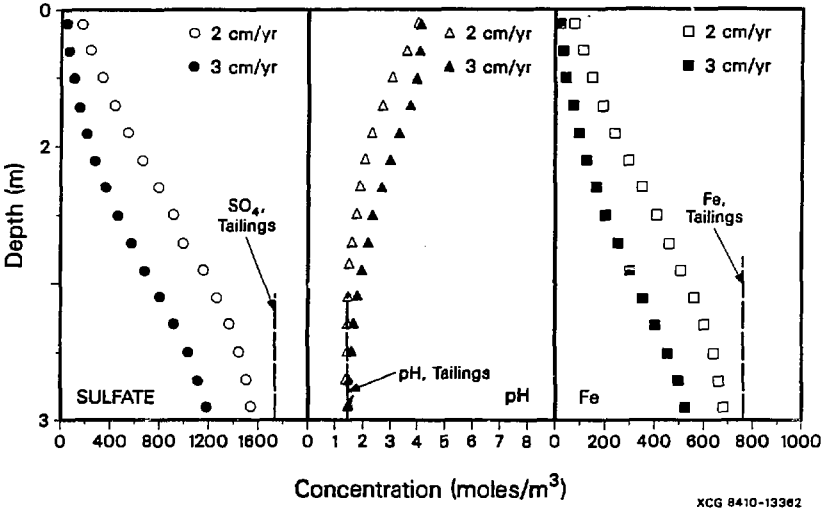

Fig. 20. Results of simulation: dilution front; comparison of effects of two different infiltration rates.

Table 2. Chemical compositions of tailings water and rain water.

Chemical species	Concentration m moles/ℓ (moles/m^3)	
	Rain water	Ground water
pH	6.0	1.43
Ca	0.0054	3.7
Mg	0.0013	78.6
Na	0.0071	8.0
K	0.0015	0.0056
Fe	0.0001	773.0
Aℓ	0.001	431.0
Si	0.001	1.53
Cℓ	0.018	3.25
C (Total Alkalinity)	0.0001	0.001
SO_4	0.0009	1757.0

As should be expected, the higher the average infiltration rate, the deeper the dilution front. In Figure 21, the results for the 2 cm/yr average annual infiltration case are compared with field data for pH, sulfate and Fe. Comparison of the pH results is quite good. As for sulfate and Fe, the field data shows a much sharper front than the more smeared computed profile. Yet the depth over which dilution has been effective is roughly the same, suggesting an overall annual average infiltration rate of 2 cm/yr.

Examination of the detailed printout from the DYNAMIX runs indicated that none of the species attained supersaturation and hence no species precipitated in the zone of dilution.

The Lower Interface Leaching Problem

The profiles of chemical species (Fig. 4) show that at Site RB the bottom meter of the tailings pile show a pronounced depletion of all chemical species. The existence of this leached zone has been difficult to interpret. One possible interpetation is that an alkaline extraction process was used at the mill during its early stages. If this were so we should expect much higher pH than observed within the shallow aquifer beneath the tailings. This interpetation therefore does not appear reasonable.

A second explanation is to consider whether the periodic rising of the water table into the bottom portion of the tailings during flooding events and the lateral flow in the capillary fringe could have flushed the bottom part of the tailings. As discussed by Narasimhan et al. (1984, Fig. 3), the bottom part of the tailings is possibly set in s trench which was cut into the soil zone.

In order to test this hypothesis of flushing out, consider the slab representing the bottom 1 m of the tailings, shown in Figure 22. Ground

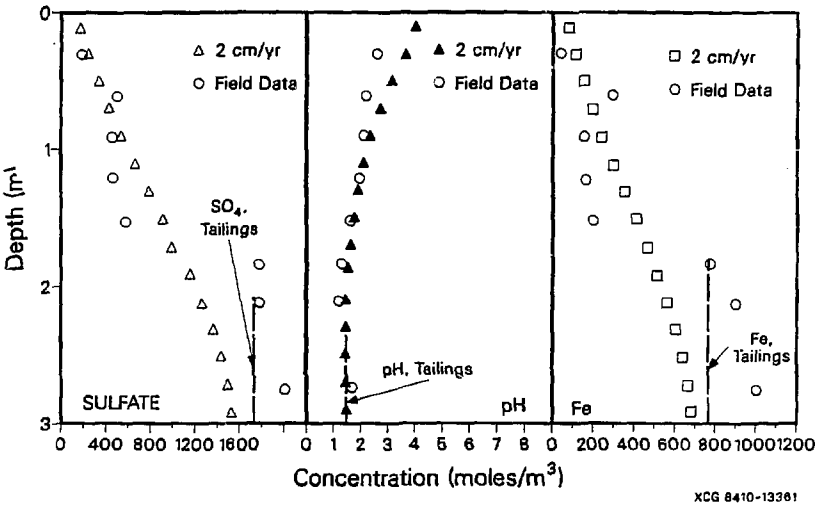

Fig. 21. Results of simulation: comparison of simulated and observed dilution profiles.

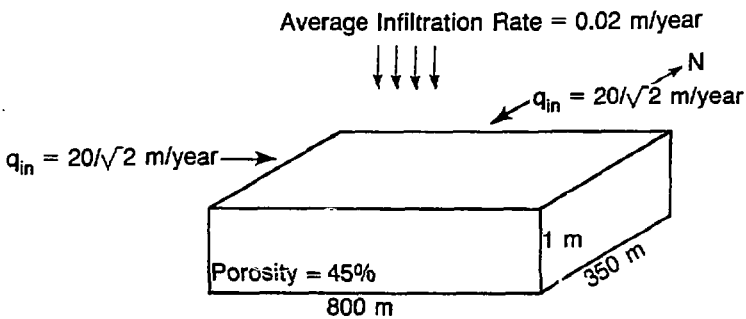

Fig. 22. Geometric set up used for analyzing the possible flushing out of lower part of tailings.

water enters the slab from the northwest at a constant rate of 20 m/yr. We assume an average vertical infiltration rate of 2 cm/yr and a porosity of 0.45 for the tailings material. Initially the tailings is filled with undiluted tailings water. We may now calculate, in a simple fashion, the number of years required to displace the tailings water by the incoming water, as follows.

Volume of water within slab $= 800 \times 350 \times 1 \times 0.45 = 1.26 \times 10^5\ m^3$

Ground water inflow $= \frac{20}{\sqrt{2}}(800 + 350) = 1.63 \times 10^4\ m^3/yr$

Infiltration per year $= 0.02\ (800)\ (350) = 5.6 \times 10^3\ m^3$

If N is the number of years needed to displace the tailings water by ground water, then,

$$(1.63 \times 10^4)\ N = 1.26 \times 10^5 + (5.6 \times 10^3)N$$

$$\text{Therefore } N = \frac{1.26 \times 10^5}{(1.63 \times 10^4 - 5.6 \times 10^3)} = 11.8 \text{ years}$$

This calculation shows that even if the bottom of the tailings is perennially flooded and has throughput of 20 m/yr ground water velocity, it will take 12 years for significant leaching to occur. The two-dimensional transect calculations (Figs. 17 through 19) show that the lateral fluxes of water in the capillary fringe are extremely small compared to the 20 m/yr ground water velocity assumed above. Thus, even if we assume that the bottom of the tailings remains flooded for an average of 4 months a year, flushing and leaching would take at least 35 years, whereas the tailings pile has remained abandoned only for about 20 years.

Thus, the possibility of flushing is also unsatisfactory. The possibility that the observed leaching is a local phenomenon, or that special initial conditions at the time of emplacement are the cause of leaching should be considered as alternative explanations.

Before concluding consideration of the leaching problem, two other possibilities should be mentioned. The first is that the regional ground water velocity is far in excess of the 20 m/yr magnitude assumed. This estimate of 20 m/yr was based on a plume distance of 1800 m over a 20 year-period (White et al., 1984). The second is that the observed leaching is purely a local phenomenon restricted to the vicinity of site RB. Of these two possibilities, it is easy to see that the second possibility can only be evaluated after further detailed field studies.

We now consider the question of regional ground water velocity in greater detail. The water table map (Fig. 3) indicates that the water table gradient immediately below the tailings, on the western side, has a maximum value of about 0.003 m/m. Let us assume that the long-term average is much higher, say, 0.01 m/m. Then, for a darcy velocity of 20 m/yr or 6.3×10^{-7} m/s, we can estimate hydraulic conductivity by the relation

$$K = \frac{q}{I} = \frac{6.3 \times 10^{-7}}{0.01} = 6.3 \times 10^{-5} \text{m/s or } 6.3 \times 10^{-3} \text{cm/s}$$

where K is hydraulic conductivity, q is darcy velocity and I is hydraulic gradient. If we were to use a gradient of 0.003, the estimate of K would be more than 3 times larger than the above estimate of 6.3×10^{-3} cm/s. The range of values of hydraulic conductivities for natural geological materials given by Freeze and Cherry (1979, p. 29) indicates that the value 6.3×10^{-3} cm/s pertains to either silty sands or clean sands.

An attempt was made by the authors in 1982 to conduct a pump test in a borehole at Site RB, which pierced the shallow aquifer. The test was soon abandoned, with production being less than 1 gal/min, declining with time. Later, Hydrogeochem of Tucson conducted a similar pump test at Site RB on

a newly constructed gravel-packed well. This well produced only about 0.88 gpm (J. Brinkman, Jacobs Engineering, personal communication, 1984) indicating a formation of fairly low permeability. These two experiences suggest that the shallow aquifer at Riverton is very heterogeneous. The geochemically derived estimate of 20 m/yr, which led to an estimate of 6.3×10^{-3} cm/s for hydraulic conductivity, is therefore most likely to be on the high side. At the present time, the possibility of long-term regional groundwater velocity being greater than 20 m/yr should indeed be taken to be very small, on the basis of current knowledge of the physical properties of the system.

The Tailings-Aquifer Mixing Problem

The geometry of the system modeled is shown schematically in Figure 23. We consider a slab of the shallow aquifer, 800 x 350 x 10 m, which has a porosity of 30%. Ground water enters from the northwest at a constant velocity of 20 m/yr. This velocity was chosen based on the present location of the contaminant plume (Narasimhan et al., 1984). The components of the ground water fluxes perpendicular to the faces of the slab are shown in the figure by arrows. Tailings water enters the system vertically at rates varying with time, as computed from Stage 1 calculations. The average composition of the ground water and the tailings water are assumed known and are tabulated in Table 3. Initially, the shallow aquifer is assumed to contain ground water. For purposes of modeling, we discretize this system into seven volume elements, each of which is a prism, with the long dimension oriented perpendicular to the direction of regional ground water flow.

We consider that the mill was active for a period of 5 years, followed by 20 years of abandonment, for a total of 25 years. We assume that the average

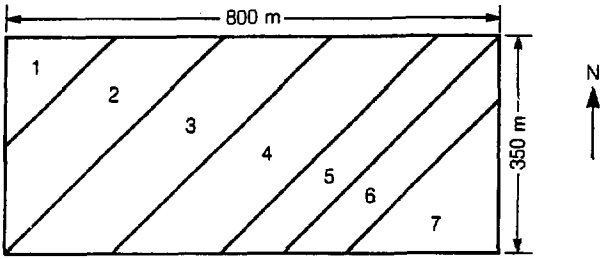

A

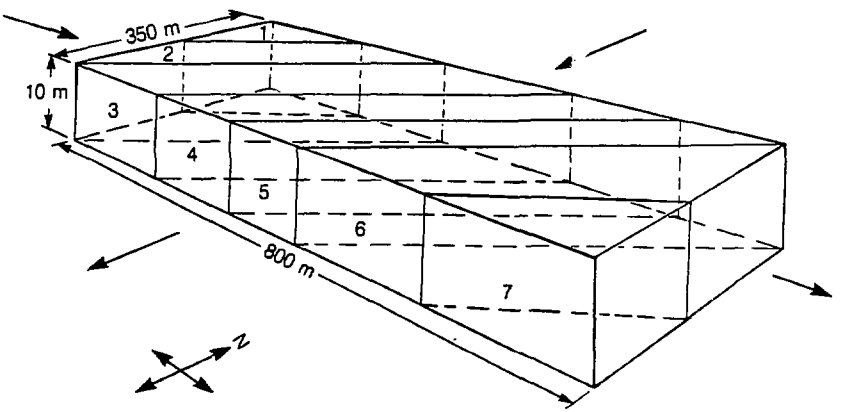

B

Fig. 23. Schematic of mesh used in the tailings-aquifer mixing calculations.

Table 3. Compositions of ground water and tailings water.

Chemical species	Concentration m moles/ℓ (moles/m^3)	
	Ground water	Tailings water
ph	7.60	1.43
Ca	1.76	3.70
Mg	0.905	78.60
Na	3.93	8.00
K	0.105	0.0056
Fe	0.003	773.00
Aℓ	0.001	431.00
Si	0.548	1.53
Cℓ	0.8174	3.25
C (Total Alkalinity)	4.73	0.001
SO_4	2.34	1757.00

annual infiltration over the tailings was 1 m/yr during the active phase; we then approximate the decline in infiltration rate during the abandoned period by the curve shown in Figure 24. This infiltration data was obtained from the 0.55X (CRAE) Case, with rainfall averaged over quarterly periods (Fig. 16).

For geochemical calculations using PHREEQE, our experience has shown that carbon should be handled as total alkalinity rather than total carbon. We assumed, based on field data, that there was an abundance of calcite buffer in the shallow aquifer and that the most important mineral species to be considered in the precipitation reactions were gypsum ($CaSO_4 \cdot 2H_2O$), gibbsite (Al_2O_3), and iron hydroxide ($Fe(OH)_3$). Based on field data (Narasimhan et al., 1984, Fig. 26), we set the calcite saturation index (Log IAP $CaCO_3$) equal to -7.6.

In general, the mixing of the shallow groundwater with the highly acidic tailings water leads to neutralization and a gradual increase in pH. Concomitantly, calcite is consumed, while gypsum, gibbsite and iron hydoxide are precipitated. The amount of gypsum precipitated is relative to the amount of calcite dissolved (and hence, the magnitudes of supersaturation of calcite as evidenced by field data). However, at the high pH of the ground water, both gibbsite and iron hydroxide are almost completely precipitated and the contaminated aqueous phase is almost totally devoid of these two species.

The evolution, in space, of the contamination within the shallow aquifer body modeled is of considerable interest. It is clear from Figure 23 that northwest of the tailings, where ground water enters the system, the ground water has maximum neutralization ability. As one proceeds downstream from volume element 1, however, the incoming fluid from the upstream element is progressively more contaminated. As a result, the magnitude of contamination increases downstream at any given instant in time.

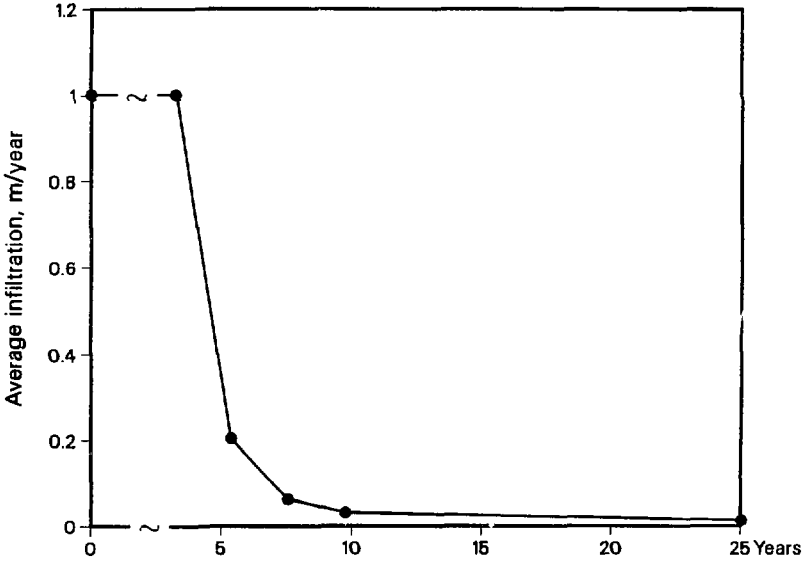

XCG 8410-13357

Fig. 24. Infiltration rate as a function of time used in tailings-aquifer mixing calculations.

This is illustrated in Figure 25, in which the concentrations of sulfate in nodes 1 thru 7 are plotted at different times. It is readily seen that the concentrations show a pronounced increase in the downstream direction. Recognizing that the contaminated water leaving volume element 7 receives no more contaminants, it is easy to visulatize that the plume is generated in the vicinity of the SE corner of the tailings and migrates towards the Little Wind River. Note in Figure 25 that the concentrations at 25 years are in excess of those at 15 years. This appears to be an oscillation in the numerical solution. Whether this oscillation is physically realistic or whether it is computational has not been studied. Nevertheless, it is clear that this oscillation does not modify the overall results.

As mentioned earlier, significant amounts of gypsum were being precipitated in elements 1 - 7 throughout the mixing history. The rate of precipitation of gypsum in moles per cubic meter of water per second is plotted as a function of time for the seven volume elements in the system in Figure 26. The precipitation rates vary from about 2×10^{-5} moles/m^3 sec to less than 1×10^{-6} moles/m^3 sec. While the precipitation rates show consistent behavior in respect to elements 2 - 7, the behavior of element 1 is some what erratic. This may be due to the computational difficulties involved in mixing two solutions of markedly different chemical composition.

The present state of the system at Riverton corresponds to the conditions at the end of 25 years of the computational problem (5 active years + 20 years of abandonment). The computed results show that at the end of 25 years the pH values varied from 6.97 at volume element 1 in the northwest to 6.53 at volume element 7 in the southeast. This range compares favorably with the valuea of 6.4 to 7.0 measured in the field (Fig. 5).

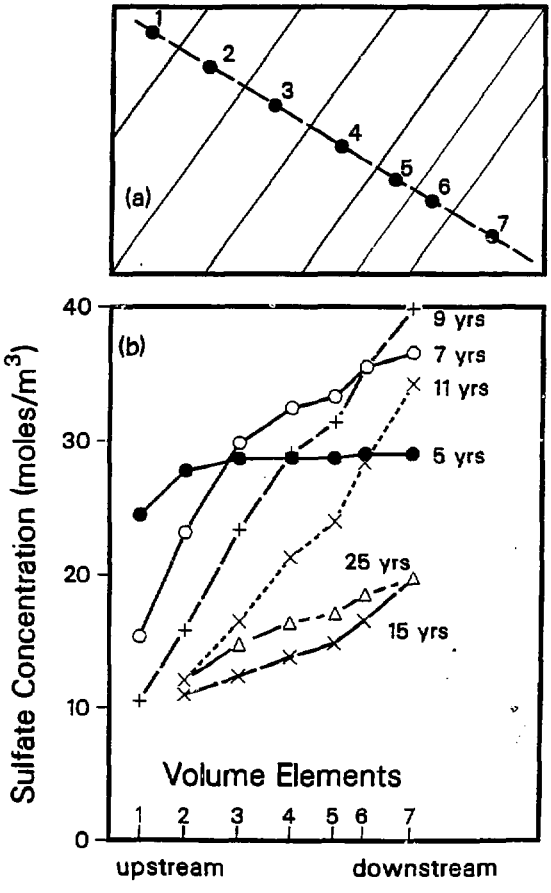

XCG 8410-13360

Fig. 25. Results of simulation: sulfate profile as a function of time within aquifer below the tailings.

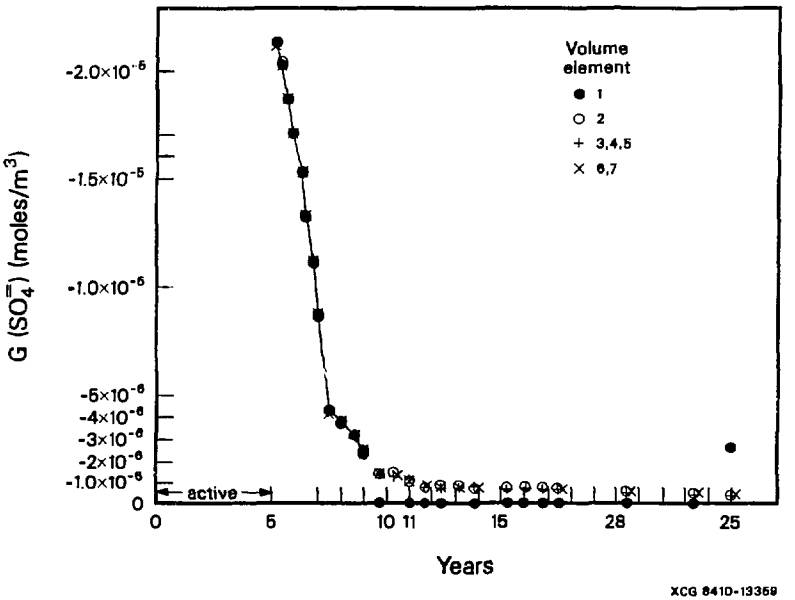

Fig. 26. Results of simulation: precipitation rates of sulfate as a function of time.

STAGE 3: THE CONTAMINANT PLUME PROBLEM

The final task in the history matching effort is to model the contaminant plume. In this regard we shall restrict our attention to the simulation of the sulfate plume. We are concerned with a flow region schematically represented by Stage 3 in Figure 8. Within this region we need to handle advection, diffusion, hydrodynamic dispersion and precipitation. The advection is further characterized by fluid fluxes that vary with time in the vertical direction. In order to handle the hydrodynamic dispersion coefficient in terms of the longitudinal coefficient, D_L, and the transverse coefficient, D_T, rather than the general tensorial quantities, D_{ij}, we shall define our mesh to consist of volume elements with nodes defined by stream lines and isopotential lines, (Fig. 27). Within the plane area of the tailings, the vertical infiltration rate times the plane area of an elemental volume yields the volumetric rate at which tailings water enters that element. We assume that the regional ground water velocity (Darcy velocity) is 20 m/yr towards the southeast. The time-dependent infiltration rates are the same as those given in Figure 24. The rates of precipitation of sulfate are the same as those given in Figure 26. We will assume that the rates of precipitation for elements 101 and 102 (Fig. 27) will be the same as those of element 1 (Fig. 26); the rates for elements 201 to 204 will be the same as those of element 2 (Fig. 26,) and so on.

For computational purposes we will assume that the shallow aquifer has a longitudinal dispersivity of 1 m and a transverse dispersivity equal to one-tenth that of the longitudinal value. We also assume that the transfer of chemical species from the tailings to the aquifer occurs by advection, hydrodynamic dispersion, and molecular diffusion. The computations were carried out with the program TRUMP.

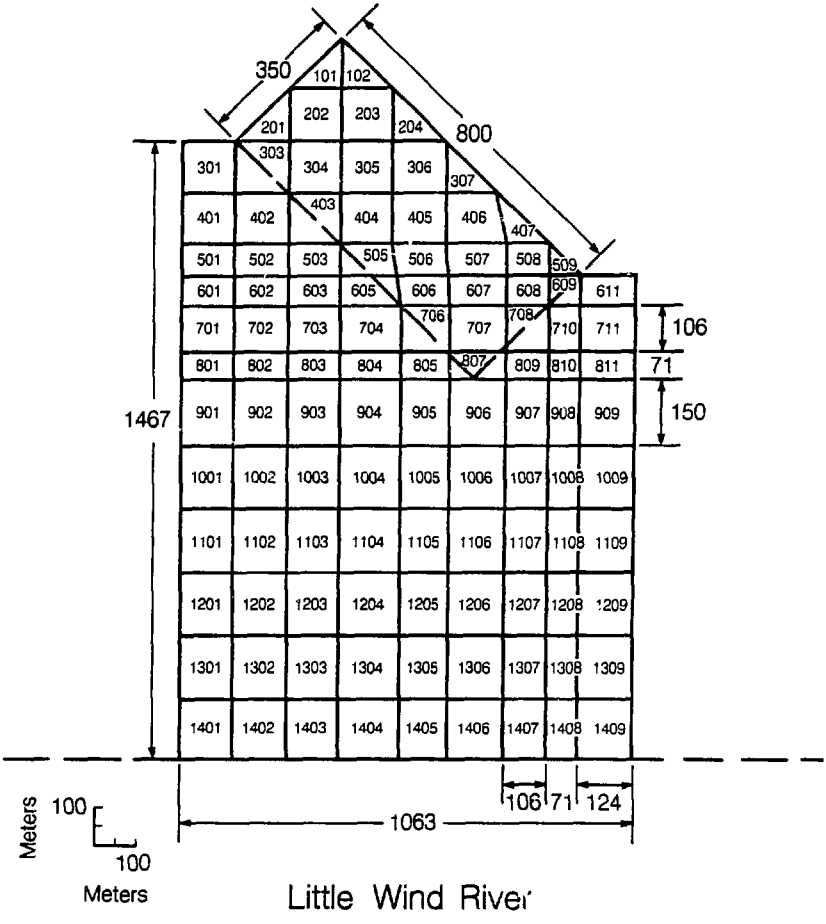

Fig. 27. Mesh used for sulfate plume simulation.

Preliminary simulation results show that negative sulfate concentrations were obtained for some of the elements, indicating that more sulfate was being precipitated than was being replenished from the tailings. This shows that the magnitude of sulfate precipitated is significant compared to the total influx of sulfate from the tailings. In order to avoid this physically unrealistic situation, the influx of sulfate from the tailings was enhanced by artificially increasing the molecular diffusion coefficient for the tailings-aquifer interaction by a small amount. This increase was decreased with time. Thus, the molecular diffusion coefficient was fixed for the first 9 years and decreased for the rest of the simulation period.

The results of this simulation yielded the evolution of the sulfate plume with time. Figure 28 shows plots of disposition of the plume (i) 2 years into the active phase; (ii) at the end of the active phase (5 years); (iii) 4 years after abandonment; and (iv) 20 years after abandonment. The figure shows how the contaminant plume might have grown and migrated in the past. It is also clear that the magnitude of contamination was much larger in the past than at the present time. The sulfate plume is currently on the wane.

In Figure 29, the computed contaminant plume at 20 years after abandonment is shown compared with the plume observed at the present time (Fig. 5). As can be seen, the observed and computed magnitudes are reasonably close, as are the patterns of the contours. Towards the river, however, the computed values reach 80 moles/m^3 while maximum observed concentrations are little more than 31 moles/m^3. For clarity, the 20 moles/m^3 contour of the computed results is shown compared with the observed 21 moles/m^3 contour in Figure 30. The comparison is remarkably good considering the extreme complexity

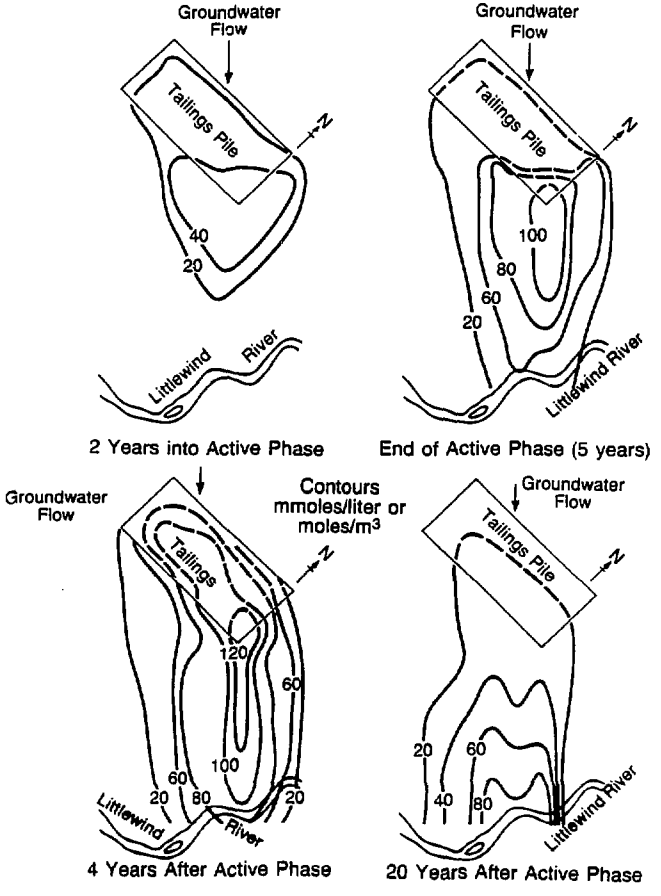

Fig. 28. Results of simulation: sulfate plume as a function of time.

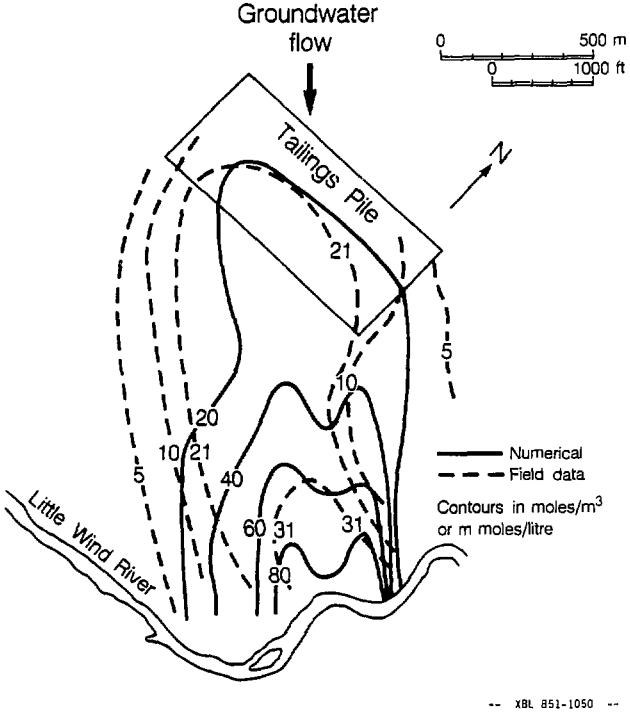

Fig. 29. Results of simulation: comparison of simulated and observed sulfate plumes.

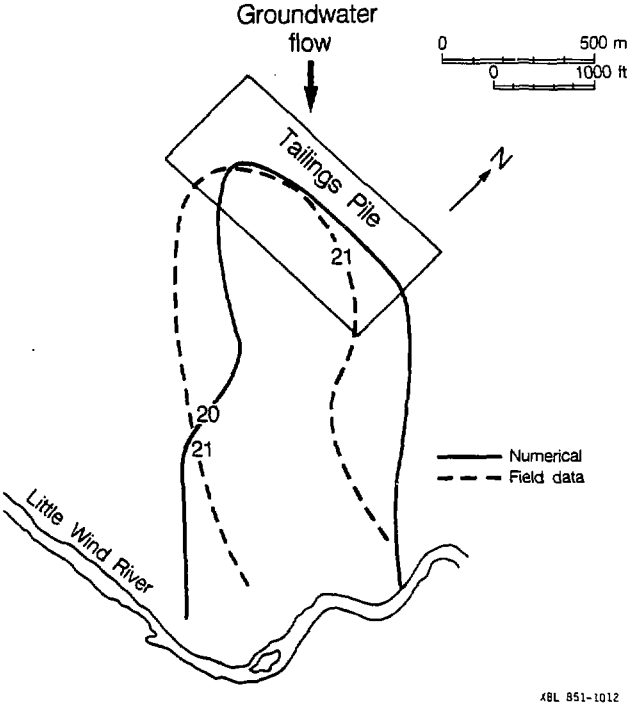

Fig. 30. Results of simulation: comparison of simulated (20m moles/liter) and observed (21 mmoles/liter) sulfate contours.

of the overall problem. It is encouraging to see that the simulated results agree reasonably well with the observed results in the region immediately below the tailings and in the near vicinity of the tailings.

The higher computed values of the maximum concentration of the plume could be due to several factors. First, the strength of the plume is primarily dictated by the very heavy influx of the tailings water during the acive phase. However, we have little data on how the pile was managed during the active phase; thus, a significant lack of knowledge exists about the initial conditions. Second, we have used a single average concentration for the tailings water. This again is gross simplification. Third, we have modeled the system such that it has a plane area of 800 by 350 m. However, we know that the eastern third of the tailings pile is much thinner than the western two-thirds. Thus, the total influx of tailings water implied in the computations is probably much higher than whst may actually be the case. If so, the plume concentrations arrived at by the computations are likely to be higher, as is indeed the case.

DISCUSSION

The three-stage sequential simulation approach followed in the present study has lead to a credible matching of the field observations through mathematical models, using observed field data as input parameters. The matched phenomena include fluid potentials as well as chemical concentrations. The methodology used clearly establishes the feasibility of simulating field systems involving hydrodynamics coupled with transient, reactive multiple-species chemical transport. The ability to achieve this has become possible only within the past few years. Our success in the present work represents only the first crude attempt at a very complex problem. The present study, it must be emphasized, has only provided proof of the concept of handling a problem involving multiple-species, reactive chemical transport. Neither sensivity analyses nor parametric studies have been carried out. Nevertheless, the dominant physicochemical mechansims governing the low-level waste migration problem have been identified. Our ability to quantify these mechanisms has been demonstrated.

Much work needs to be done to validate the model and benchmark it for licensing purposes. In addition, sensitivity analyses and parametric studies have to be carried out to predict the future response of the system and to devise proper remedial measures.

Program DYNAMIX as it exists now is only a prototype research tool. As such it is not in a form suitable for distribution. In its present form the coupling between the transport part of the code and PHREEQE is computationally inefficient. Literally, the PHREEQE code is called in total for every reaction calculation. This brute force approach had to be taken due to

time constraints involved in the project goals. By carefully blending the PHREEQE computational model into the transport code, one should be able to greatly speed up the computing effort. For a single time step, per volume element, the DYNAMIX Code currently requires about 1.5 cpu seconds on the CDC 7600 machine.

Another factor that tends to slow down the progress of the problem in real time is that the explicit method is currently being used in DYNAMIX for marching in the time domain. This could be overcome by choosing the implicit mode of calculations. Although this extension to the implicit mode (Crank-Nicolson; backward differencing) is not difficult in principle, it is essential to conceptually understand the logic that is involved in volumetrically mixing waters of different chemical qualities. To wit, given a certain interval of time, what is the correct size of the volume element over which complete mixing can be assumed? How do molecular diffusion and hydrodynamic dispersion influence the logic for mixing?

Third, the PHREEQE code as used in DYNAMIX considers the mixing of only the aqueous phases at low temperatures. The code needs to be extended to include the interaction with the solid phase in such a fashion that the genesis or the consumption of specific mineral species can be followed.

The problem of abandoned uranium mill tailings is characterized especially by the partially saturated tailings material. The role of free oxygen in controlling the water-solid interaction is extremely important in the unsaturated zone. There is a basic need to extend the PHREEQE algorithms to effectively handle this problem.

With the incorporation of the improvements discussed above, the DYNAMIX algorithm would become a viable and practical tool in quantifying and predicting

the transport of heavy metals and other chemical species in groundwater systems. Such a tool would be of considerable use in dealing with the management, not only of uranium mill tailings, but also of other sources of contamination, such as copper mill tailings, sanitary land fills and waste ponds. Additionally, the DYNAMIX model will also be directly applicable to generation and transport of acids in the soil (the acid rain problem) or the leaching and enrichment of useful metals in and around the zone of weathering (the supergene sulfide enrichment problem).

REFERENCES

Edwards, A. L., 1972. TRUMP: A Computer Program for Transient and Steady State Temperature Distributions in Multi-dimensional Systems, Report No. 14754, Rev. 3, Lawrence Livermore National Laboratory.

Freeze, R. A., and J. A. Cherry, 1979. Groundwater, Prentice Hall, New Jersey.

Luthin, J. N., and P. R. Day, 1955. Lateral Flow Above a Sloping Water Table, Soil Sci. Soc. Am. Proc., 18, 406-410.

Morton, F. I., 1978. Estimating Evaporation from Potential Evaporation Practicality of an Iconoclastic Approach, Jour. Hydrology, 38, 1-32.

Narasimhan, T. N., A. F. White, A. R. Smith and T. Tokunaga, 1984. Hydrology and Geochemistry of the Uranium Mill Tailings Pile at Riverton, Wyoming Part I. Field Data, Lawrence Berkeley Labortory Report No. 18525, Berkeley, California.

Narasimhan, T. N. and P. A. Witherspoon, 1976. An Integrated Finite Difference Method for Analyzing Fluid Flow in Porous Media, Water Resources Res., 12(1), 57-64.

Narasimhan, T. N., and P. A. Witherspoon, 1978. Numerical Model for Saturated-Unsaturated Flow in Deformable Porous Media, Part 3. Application, Water Resources Res., 16(6), 1017-1034.

Narasimhan, T. N., P. A. Witherspoon and A. L. Edwards, 1978. Numerical Model for Saturated-Unsaturated Flow in Deformable Porous Media, Part 2. The Algorithm, Water Resources Res., 16(2), 255-261.

Narasimhan, T. N., and P. A. Witherspoon, 1977. Numerical Model for Saturated-Unsaturated Flow in Deformable Porous Media, Part 1. Theory, Water Resources Res., 13(3), 657-666.

Parkhurst, D. L., D. C. Thorstensen, and L. N. Plummer, 1980. PHREEQE - A Computer Program for Geochemical Calculation, U.S. Geological Survey, Report of Investigation, 80-96.

Rasmuson, A., T. N. Naraaimhan and I. Neretnieks, 1982. Chemical Transport in a Fissured Rock, Validation of a Numerical Model, Water Resources Res., 18(5), 1479-1492.

Reisenauer, A. E., K. T. Key, T. N. Narasimhan, R. W. Nelson, 1982. TRUST: A Computer Program for Variably Saturated Flow in Multi-Dimensional Deformable Media, U.S. Nuclear Regulatory commission, NUREA/CR-230.

Staple, W. J., 1974. Modified Penman Equation to Provide the Upper Boundary Condition Computing Evaporation for Soil, Soil Sci. Soc. Am. Proc., 38, 837-839.